

The effects of turbulent mixing on the correlation between two species and on concentration fluctuations in non-premixed reacting flows

By SATORU KOMORI¹, J. C. R. HUNT², TAKAO KANZAKI¹
AND Y. MURAKAMI¹

¹ Department of Chemical Engineering, Kyushu University, Hakozaki, Fukuoka 812, Japan

² Department of Applied Mathematics and Theoretical Physics, University of Cambridge,
Silver Street, Cambridge CB3 9EW, UK

(Received 1 June 1989 and in revised form 20 December 1990)

When two species A and B are introduced through different parts of the bounding surface into a region of turbulent flow, molecules of A and B are brought together by the combined actions of the turbulent velocity field and molecular diffusion. A random flight model is developed to simulate the relative motion of pairs of fluid elements and random motions of the molecules, based on the models of Durbin (1980) and Sawford & Hunt (1986). The model is used to estimate the cross-correlation between fluctuating concentrations of A and B , $\overline{c_A c_B}$, at a point, in non-premixed homogeneous turbulence with a moderately fast or slow second-order chemical reaction. The correlation indicates the effects of turbulent and molecular mixing on the mean chemical reaction rate, and it is commonly expressed as the 'segregation' or 'unmixedness' parameter $\alpha (= \overline{c_A c_B} / \overline{C_A} \overline{C_B})$ when normalized by the mean concentrations $\overline{C_A}$ and $\overline{C_B}$. It is found that α increases from near -1 to zero with the time (or distance) from the moment (or location) of release of two species in high-Reynolds-number flow. Also, the model (and experiments) agrees with the exact results of Danckwerts (1952) that $\overline{c_A c_B} / (\overline{c_A^2} \overline{c_B^2})^{1/2} = -1$ for mixing without reaction. The model is then extended to account for the effects on the segregation parameter α of chemical reactions between A and B . This leads to α eventually decreasing, depending on the relative timescales for turbulent mixing and for chemical reaction (i.e. the Damköhler number). The model also indicates how a number of other parameters such as the turbulent scales, the Schmidt number, the ratio of initial concentrations of two reactants and the mean shear affect the segregation parameter α .

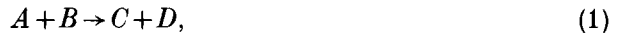
The model explains the measurements of α in previously published studies by ourselves and other authors, for mixing with and without reactions, provided that the reaction rate is not very fast. Also the model is only strictly applicable for a limited mixing time t , such that $t \lesssim T_L$ where T_L is the Lagrangian timescale, because the model requires that the interface between A and B is effectively continuous and thin, even if highly convoluted. Flow visualization results are presented, which are consistent with the physical idea underlying the two-particle model.

1. Introduction

In most fluid flows where there are chemical reactions, the different species are introduced separately into the flow and so have to be mixed by turbulence and molecular motion. This mixing and reaction determine the distribution of chemical

pollutants in the atmospheric boundary-layer flow and the effectiveness of turbulent combustion or chemical reactions in many industrial processes. Such processes are also critical in the atmospheric environment where they affect the chemical transformations of exhaust gases from automobiles and power plants and the formation of acid rain. A better understanding of these reactive-diffusive flows should improve the engineering design of many chemical and energy processes, and the rational determination of acceptable kinds of emissions into the atmosphere in different conditions and locations.

When considering the one-step irreversible, second-order chemical reaction between chemical species A and B in an isothermal flow,



a general turbulent diffusion (mass-conservation) equation can be written for the mean concentration \bar{C} of A or B :

$$\frac{\partial \bar{C}}{\partial t} + \bar{U}_i \frac{\partial \bar{C}}{\partial x_i} = \frac{\partial [\kappa(\partial \bar{C} / \partial x_i) - \overline{u_i c}]}{\partial x_i} - k[\bar{C}_A \bar{C}_B + \overline{c_A c_B}], \quad (2)$$

where C and c are the instantaneous and fluctuating concentrations, U_i and u_i the instantaneous and fluctuating velocities in the x_i -direction, respectively, κ the molecular diffusivity, k the chemical reaction rate constant and the overbars indicate mean (averaged) values. The second term on the right is the mean chemical reaction rate term, and it can be split into the mean concentration product $\bar{C}_A \bar{C}_B$ and the concentration fluctuation product $\overline{c_A c_B}$. Clearly, the latter correlation between the species concentration fluctuations, $\overline{c_A c_B}$, (first introduced by Danckwerts 1952) is of great importance, if the segregation parameter α ($= \overline{c_A c_B} / \bar{C}_A \bar{C}_B$) is not equal to zero. (Note that if $\alpha = -1$, there is no molecular mixing because $\overline{C_A C_B} = 0$.) In this sense, it is interesting to estimate α for a moderately fast reaction in which the reaction time is comparable with the mixing time. For other kinds of reactions other statistical quantities involving C_A and C_B are required, but some understanding of these quantities can be derived from the theory and physical arguments for α , which we concentrate on in this paper.

In many studies of chemical processes in the atmosphere, such as numerical simulation of the atmospheric diffusion of chemical pollutants, the correlation of the concentration fluctuation $\overline{c_A c_B}$ has been surprisingly neglected, and even in studies of chemical reactors with a moderately fast reaction plausible assumptions such as Toor's hypothesis (Toor 1969) have been used. Thus, the concentration correlation has not been discussed explicitly in any detail. However, more recently Komori & Ueda (1984), Mudford & Bilger (1984), Bennani, Gence & Mathieu (1985), Saetran *et al.* (1989) and others have measured $\overline{c_A c_B}$ in laboratory experiments of non-premixed turbulent reacting flows with a moderately fast or slow second-order chemical reaction. They showed that $\overline{c_A c_B}$ is not negligible compared with the mean concentration product $\bar{C}_A \bar{C}_B$, and, if it is neglected, it can cause serious errors in the estimation of the mean chemical reaction rate. However, the experiments differed considerably in their measurements of $\overline{c_A c_B}$; even differing in the sign of α . The large difference between the previous measurements have given rise to some controversy (Bilger, Mudford & Atkinson 1985). In some quite different, but related experiments, Warhaft (1984) studied the mixing between matter and heat released from two small sources, with a spacing between them, in turbulent flows. He showed how α changes sign downwind of the source. No theoretical and physical arguments have yet been put forward to relate all these observations - we shall attempt to do so here.

Direct numerical simulations of the full equation is the only complete computational approach; Riley, Metcalfe & Orszag (1986) predicted the concentration statistics in a turbulent mixing layer with a second-order chemical reaction. Picart, Chollet & Borghi (1989) computed concentration statistics in a decaying isotropic and homogeneous turbulence of Warhaft (1984). However, the direct simulations are limited to very low-Reynolds-number flows of order of 10^2 and they have not been able to explain the eddy motions with small scales comparable to the Kolmogorov scale, which play an important role in reacting flows. These motions often results in unsymmetrical profiles of the mean quantities in the symmetrical concentration field. Therefore, two types of turbulence models have been developed for turbulent reacting flows, and the details have been reviewed by Libby & Williams (1980) and Pope (1985). Most of the models are based on the conventional methods of turbulence closure but they cannot predict the correlation $\overline{c_A c_B}$ without further closure assumptions, such as taking α equal to a constant. At present, it is not possible to derive the concentration correlation from conventional models, because of the lack of conclusive measurements.

Another type of model is based on computing the evolution of the probability density function (p.d.f.) for the concentrations of A and B . As Pope (1985) remarks in his lengthy review, most of these (p.d.f.) methods involve some assumptions about diffusion and mixing processes, and their scales for these processes are essential inputs to the transport equations for the joint p.d.f. for the species concentrations. (Some of the physical concepts leading to the model equations are not discussed.) It is possible with the p.d.f. model to predict $\overline{c_A c_B}$ exactly, since it does not need a closure assumption if the molecular mixing term can be neglected. Such models use an Eulerian formulation but some of the mixing terms are based on Lagrangian concepts, e.g. see Curl (1963). However, the connection between fluid motions and mixing processes is far from clear, so such models give little insight into the physical processes controlling mixing and reactions although they are proving to be rather successful in modelling many reacting flows. In fact, Arrojo *et al.* (1988) recently presented interesting calculations by solving p.d.f. equations by means of a Monte Carlo technique.

On the other hand, a p.d.f. model based on a Lagrangian formulation can be postulated by using a comparatively simple stochastic equation, such as a Langevin equation, for modelling the fluid particle motions. Such a model avoids solving a complicated transport equation for the p.d.f. Moreover, the model affords a clearer physical interpretation than the Eulerian model (Pope 1985). Chung (1976) has conducted calculations of both diffusion flames and a plane shear-free layer by using the p.d.f. equations based on the Langevin equation, but he has not presented details about the chemical reaction rate and the concentration fluctuation correlation term. Thus, a p.d.f. model, based on a Lagrangian formulation, has not yet been developed for turbulent reacting flows. It appears that such models are based on the idea of mixing being determined by the displacement statistics of a single fluid element and mixing with the mean environment. This cannot lead to a general model for concentration fluctuations and mixing. Considering this point, Durbin (1989) has very recently developed his Lagrangian stochastic model (Durbin 1980) for a reacting flow with an infinite reaction rate constant, but he has not yet developed it for a moderately fast or slow reaction.

The fundamental concepts about mixing and reactions reviewed by Hill (1976), Bourne *et al.* (1981) and Broadwell & Breidenthal (1982) have been mainly concerned with the microscopic processes of molecular diffusion and reaction across sheets of

high concentration gradients as they undergo stretching and random distortion by particular kinds of eddying motions and large-scale coherent structures. After identifying some specific mechanisms, these authors have developed some quantitative predictions about mixing and reactions, but they have not predicted or discerned how the segregation parameter α varies in different flows and different reactions.

The purposes of this study are to review the previous measurements of the concentration fluctuation correlation, i.e. the segregation parameter, obtained in non-premixed reacting flows with a moderately fast or slow second-order chemical reaction, and then to develop a Lagrangian stochastic model which can explain the previous measurements, and which helps to define the essential parameters for non-premixed reacting flows. This paper concentrates mainly on discussing the segregation parameter α , or the intensity of segregation, defined by the ratio of the concentration fluctuation correlation $\overline{c_A c_B}$ to the mean concentration product $\overline{C_A C_B}$, because of its special practical importance, as mentioned above. But we also consider the correlation coefficient $\overline{c_A c_B} / c'_A c'_B$ where c'_A and c'_B are the r.m.s. values of c_A and c_B , because in certain circumstances this is a constant in a non-reacting flow, which provides a strong check on models and experiments.

First, a brief review is given in §2 of the previous measurements of the segregation parameter α which differ from one another. In §3, a Lagrangian stochastic model which is applicable to non-premixed homogeneous flows with second-order reactions is developed from the marked-particle-pair trajectory model of Sawford & Hunt (1986). Computations from this model have been compared with measurements of mean-square fluctuations c_A^2 for a single species released from a small single source and multiple sources in homogeneous turbulent non-reacting flows with and without mean shear (see the review by Sawford 1985). Preliminary computations of $\overline{C_A C_B}$ for two line sources of A and B in non-reacting flows by this model have also been reported by Sawford (1985). The model is used here to explain the previously published measurements of α in reacting flows. We give explanations for the effects of turbulent scales, shear, molecular diffusivity, rate of reaction and the initial concentrations of the species in non-premixed reacting flows and make comparisons between the computed α and the measurements (§4).

2. Review of the previous measurements of the segregation parameter α

There have been several notable experiments on non-premixed reacting flows in connection with the environment and combustion problems. But in only a few have there been measurements of the concentration fluctuation correlation $\overline{c_A c_B}$ and the mean chemical reaction rate in a moderately fast or slow reaction. The previous investigators and their measurements of the segregation parameter, α ($= \overline{c_A c_B} / \overline{C_A C_B}$), are listed in table 1. Komori & Ueda (1984) used a second-order chemical reaction between ozone (O_3) and nitric oxide (NO), and have estimated α both in a non-premixed reacting plume in grid-generated turbulence and in a non-premixed reacting jet with a slow uniform non-turbulent co-flow. Their estimation method was not based on the direct measurement of concentration fluctuations c_A and c_B , and α was obtained from comparisons of measurements of the mean concentrations $\overline{C_A}$ and $\overline{C_B}$, with the numerical solutions of $\overline{C_A}$ and $\overline{C_B}$ in the mass-conservation equation (2), on the assumptions of $\overline{c_A c_B} = \alpha \overline{C_A C_B}$ and gradient diffusion. Therefore, the assumption that α is constant only gives an approximate average value of α over the whole region of the flow. On this basis Komori & Ueda's (1984) results have showed

Investigators				
Komori & Ueda (1984)		Mudford & Bilger (1984)	Komori <i>et al.</i> (1985)	Bennani <i>et al.</i> (1985)
Flow configuration				
Round plume in grid-generated turbulence (in gases)	Round jet in non-turbulent co-flow (in gases)	Counter jets in a turbulent smog chamber (in gases)	Two-dimensional plume in the atmospheric surface layer (in gases)	Homogeneous plume in grid-generated turbulence (in liquids)
Chemical reaction				
NO + O ₃ → NO ₂ + O ₂	NO + O ₃ → NO ₂ + O ₂	NO + O ₃ → NO ₂ + O ₂	NO + O ₃ → NO ₂ + O ₂	HCOOCH ₃ + NaOH → HCOONa + CH ₃ OH
α				
20	1.5	-0.01—-0.67	-0.025—-0.27	-0.7
TABLE 1. Flow configuration, chemical reaction and measured values of the segregation parameter α from previous experiments				

that the approximate values of α were 20 and 1.5 in grid-generated turbulence and in a jet, respectively.

On the other hand, Mudford & Bilger (1984) have conducted their experiments in non-premixed reacting counter jets with rather special mixing and flow configuration in a big smog chamber. Because the turbulent eddies had a large enough scale in their flow, they could directly measure the concentration fluctuations of NO and O₃ by means of a gas-sampling technique. Their results have showed that the value of α ranges from -0.01 to -0.67 and is likely to take a smaller value at the initial mixing stage (in the region with small values of x in table 1 of Mudford & Bilger 1984), than in the developed mixing region. Quite recently, SaeTRAN *et al.* (1989) have measured α by using the same measuring technique at one streamwise location of a reacting mixing layer in grid turbulence. Though the comparison between the spatial and time resolutions of their gas-sampling method and Kolmogorov scales is not explicitly shown, they also obtained a negative value for α of about -0.25 in the central region of the mixing layer.

Further, Bilger *et al.* (1985) have criticized the large positive values of α obtained by Komori & Ueda (1984). According to both their analyses and the measurements of Mudford & Bilger (1984), they insisted that α should be negative in simple non-premixed flows, and the positive α of Komori & Ueda (1984) can only be attributed to their measurement errors. Certainly, Komori & Ueda's (1984) experimental data are suspect, since the correlation of the concentration fluctuations should usually be negative in non-premixed flows of only two species (with the same diffusivity) being homogeneously diluted (see §4.3.1). However, even if their measurements involve some errors, it is difficult to concede that the errors are large enough to change the sign of α . What is wrong in Komori & Ueda's (1984) experiments? An answer to this question will be given in §4.4.

To directly measure the concentration correlation, Komori, Ueda & Tsukushi (1985) have conducted field measurements in a two-dimensional reacting plume of the atmospheric surface-layer flow (sea breeze) with turbulent scales larger than those of Mudford & Bilger's (1984) counter jets. They arranged a line source with a length of 100 m at a vertical elevation of 1.5 m from the ground and emitted diluted

nitric oxide from the source. The concentration fluctuations of NO and O₃ could be measured at a height of approximately 1.5 m and distances of 35 and 100 m downstream of the line source. In this case, the turbulent eddy scale was so large that it enabled the authors to measure directly the concentration fluctuations within small errors. The results of Komori *et al.* (1985) have shown that the measured values of α ranged from -0.025 to -0.27 .

Bennani *et al.* (1985) used a liquid-phase chemical reaction between methylformate (HCOOCH₃) and sodium hydroxide (NaOH) in grid-generated turbulent flow with a high Schmidt number $Sc (= \nu/\kappa)$ of 700, emitting HCOOCH₃ from the many injectors distributed regularly on the rods of the grid into an aqueous solution of NaOH which flowed through the grid. They only measured the concentration of one chemical species NaOH, and indirectly estimated $\overline{c_A c_B}$ on the assumption that the mean velocity and concentration fields are homogeneous over the cross-section of a water tunnel. The estimated α was equal to -0.7 throughout the measurement region and its negative value was rather smaller than α in the low-Schmidt-number flows of Mudford & Bilger (1984) and Komori *et al.* (1985). The difference between liquid and gaseous flows is interesting.

Measurements to show how $\overline{c_A c_B}$ varies with the time of mixing between two species introduced into grid-generated turbulent flows have been made by Warhaft (1984) and Komori *et al.* (1989) in non-reacting flows. Warhaft (1984) studied diffusion and mixing by two experiments: in the first heat was released from two line sources heated to different temperatures θ_1 and θ_2 , and in the second heat and helium were released from a line and a point source. It should be noted that these flows contained uncontaminated air in addition to the two contaminating species. He found that near the sources $\overline{c_A c_B}$ is negative and further downwind (corresponding to a mixing time of about one Lagrangian timescale T_L) it becomes positive. He expressed the measurements as a statistical correlation $R_{AB} (= \overline{c_A c_B} / \overline{c'_A c'_B})$ rather than $\alpha (= \overline{c_A c_B} / \overline{C_A C_B})$, and found that for $t > T_L$, R_{AB} tended to a constant value of about 0.3. (In this case, on the centreline α changed from -1 to a value much larger than 1.0.)

More recently, Komori *et al.* (1989) developed a combined laser-induced fluorescence and laser scattering technique and measured the instantaneous concentrations of two species released from two plane sources separated by a splitter plate in grid-generated turbulence by using the technique which will be introduced in §4.4. Although Komori *et al.* (1989) showed only the correlation of the concentration fluctuations in their paper, α converted from the correlation grew from -1 to zero with mixing time. These experiments seem to give a clue as to why different values of α may correspond to different mixing times, and different kinds of flow.

From the above measurements we particularly seek to understand the effects of the following:

- (i) the scales of turbulence on the mixing and reaction;
- (ii) the mean shear on the mixing and reaction;
- (iii) the Schmidt number (molecular motion);
- (iv) the reaction rate constant;
- (v) the initial concentrations.

3. Lagrangian stochastic model for non-premixed reacting flows

3.1. A Lagrangian stochastic model

In reacting flows with a second-order chemical reaction, the chemical reactants are carried and mixed mainly by turbulent motions and the reaction proceeds rapidly at the interface of two reactive fluid elements by molecular diffusion. Therefore, we have to develop a theoretical model that can describe both turbulent and molecular motions. One approach is to compute directly the governing equations of the fluid flow. But this is enormously time consuming and probably wasteful, because we already know a good deal about the statistics governing the diffusion of fluid elements or particles in turbulent flow. To exploit this knowledge, Durbin (1980) developed a stochastic model for the mean and mean square of a concentration field based on the established statistics of single particles and pairs of particles in turbulent flows. Durbin's model accounted for mixing between pairs of particles by molecular diffusion, but it was assumed that the Reynolds number were high enough (though unspecified) for the rate of mixing to be independent of the values of the molecular diffusivity. Sawford & Hunt (1986) have modelled molecular diffusion explicitly by considering the displacement of very small marked particles (which might be thought of as molecules) of the species introduced into the flow which have a random thermal or Brownian motion relative to the fluid continuum. (Their calculations reduce to Durbin's in the limit of high enough Péclet and Reynolds numbers.) Here, we extend the Sawford-Hunt (1986) model to describe non-premixed reacting turbulence. The model treats only one component (the z -direction) of the displacement in a three-dimensional velocity field, and it is applied to a horizontally homogeneous flow.

Formally the mathematical problem of mixing and reaction of two species across an initially flat interface can be stated as

$$\frac{\partial C_A}{\partial t} + (u_i + U_i) \frac{\partial C_A}{\partial x_i} = \kappa \nabla^2 C_A - k C_A C_B, \tag{3a}$$

$$\frac{\partial C_B}{\partial t} + (u_i + U_i) \frac{\partial C_B}{\partial x_i} = \kappa \nabla^2 C_B - k C_A C_B, \tag{3b}$$

where

$$C_A = \begin{cases} C_{A0} & z > 0 \\ 0 & z < 0, \end{cases} \quad C_B = \begin{cases} 0 & z > 0 \\ C_{B0} & z < 0 \end{cases} \quad \text{at } t = 0.$$

The mean velocity is $U_i = (U(z), 0, 0)$ and the homogeneous turbulence is $u_i(\mathbf{x}, t)$. (Note that $\overline{u_i} = 0$). For simplicity it is assumed that the diffusivity κ and the reaction rate constant k are the same for both species. The concentrations are considered to be dilute so that the product of reaction does not affect the above equation.

According to the statistical theory of marked particles, (hereinafter we consider very small marked particles which may be thought of as molecules), the ensemble mean concentration is

$$\overline{C(z, t)} = \int_{-\infty}^{\infty} P_1(z'_1, 0; z, t) C_0^{(1)}(z'_1) dz'_1, \tag{4}$$

and the ensemble mean-square concentration at a single time and position is

$$\begin{aligned} \overline{C^2(z, t)} &= \overline{C^{(1)}(z, t) C^{(2)}(z, t)} \\ &= \int_{-\infty}^{\infty} \int_{-\infty}^{\infty} P_2(z'_1, z'_2, 0; z, z, t) C_0^{(1)}(z'_1) C_0^{(2)}(z'_2) dz'_1 dz'_2, \end{aligned} \tag{5}$$

if the separation of the two particles vanishes at a time t . Here, P_1 and P_2 are one- and two-point displacement p.d.f.'s and $C_0^{(i)}(z'_i)$ is the source distribution of particle i at a time $t = 0$ and position $z = z'_i$. For statistically stationary motions of the particles, the concept of reversed dispersion can be applied (Corrsin 1952; Sawford 1984). Therefore, the particle displacement p.d.f.'s are rewritten as

$$P_1(z'_1, 0; z, t) = P_1(z'_1, t; z, 0), \quad (6a)$$

$$P_2(z'_1, z'_2, 0; z, z, t) = P_2(z'_1, z'_2, t; z, z, 0). \quad (6b)$$

Then, we obtain

$$\overline{C(z, t)} = \int_{-\infty}^{\infty} P_1(z'_1, t; z, 0) C_0^{(1)}(z'_1) dz'_1, \quad (7)$$

$$\begin{aligned} \overline{C^2(z, t)} &= \overline{C^{(1)}(z, t) C^{(2)}(z, t)} \\ &= \int_{-\infty}^{\infty} \int_{-\infty}^{\infty} P_2(z'_1, z'_2, t; z, z, 0) C_0^{(1)}(z'_1) C_0^{(2)}(z'_2) dz'_1 dz'_2. \end{aligned} \quad (8)$$

If the initial concentrations of A and B are C_{A0} and C_{B0} , and if they are non-premixed $\overline{C_{A0}(z') C_{B0}(z')} = 0$ at $t = 0$, then from (5) and (8) with $C_A C_B$ replacing C^2

$$\overline{C_A C_B(z, t)} = \frac{1}{2} [\overline{C_A^{(1)}(z, t) C_B^{(2)}(z, t)} + \overline{C_A^{(2)}(z, t) C_B^{(1)}(z, t)}]. \quad (9)$$

Here, a marked particle is assumed to have one chemical component. If an exact specification of P_1 and P_2 can be found, (7)–(9) give exact concentration statistics. However, there is no analytically or computationally efficient method for obtaining exact solutions of these p.d.f.'s.

Sawford & Hunt (1986), following Saffman (1960), partitioned the particle displacement into a turbulent part (due to the motion of turbulent fluid particle elements containing very small marked particles at that time), and a random Brownian component (due to molecular motion), as

$$dz = w_p dt + (2\kappa)^{\frac{1}{2}} dW_a, \quad (10)$$

where w_p is the velocity of the fluid element containing the small marked particle at the given instant, and dW_a is a Gaussian white noise process. Here, the assumption that the Brownian (molecular) motion is independent of the turbulent motion is, of course, used.

We also postulate model equations for the rate of separation of pairs of particles (based on the Richardson's hypothesis that the rate of separation is a function of the instantaneous value of the separation)

$$d\Delta = R^{\frac{1}{2}}(\Delta) U^{(2)} dt + \kappa^{\frac{1}{2}} dW_d^{(2)}, \quad (11)$$

and for the displacement of the centre of mass of the two particles

$$d\Sigma = [2 - R(\Delta)]^{\frac{1}{2}} U^{(1)} dt + \kappa^{\frac{1}{2}} dW_d^{(1)}, \quad (12)$$

where Δ is the separation of two small particles, $\Delta = (z_1 - z_2)/\sqrt{2}$, $\Sigma = (z_1 + z_2)/\sqrt{2}$, $R(\Delta)$ the Eulerian structure function, and $U^{(i)}$ is the independent random velocity of particle i which is the solution of the Uhlenbeck–Ornstein process:

$$dU^{(i)} = -[U^{(i)}/T_L] dt + \sigma_w [2/T_L]^{\frac{1}{2}} dW_i; \quad U_{t=0}^{(i)} = \sigma_w N. \quad (13)$$

Here, T_L is the Lagrangian integral timescale, which is assumed to be proportional to the ratio of the turbulent integral space scale L to the r.m.s. fluctuating velocity

σ_w, dW_t is a Gaussian white noise process, and N is a zero-mean, standard Gaussian random variable. This equation is equivalent to the Langevin equation when dt approaches zero. It is well established that the equation can describe the random velocity of a single particle in homogeneous turbulence (Taylor 1921), but the use of (11) to model pairs of particles is controversial. Thomson (1986) has argued that it probably underestimates dA/dt . But it has been used in previous simulations for a single species, where there has been good agreement with experiments.

The structure function $R(\Delta)$ in (11) and (12) is an important function that determines the separation of two particles and is given by Sawford & Hunt (1986) based on Kolmogorov's results as

$$R(\Delta) = \left[\frac{\Delta^2}{L^2 + \Delta^2} \right]^{\frac{1}{3}} \left[\frac{\Delta^2}{\eta^2/\phi^3 + \Delta^2} \right]^{\frac{2}{3}}, \tag{14a}$$

where η is the Kolmogorov scale, $(\nu^3/\epsilon)^{\frac{1}{4}}$, determined by the viscous dissipation ϵ and kinematic viscosity ν , and ϕ is a constant which is equal to 0.358 (Sawford & Hunt 1986). (It is chosen to ensure agreement with Saffman's (1960) exact result for the displacement of molecules very near a source.) In the presence of mean shear, the relative streamwise displacement of a particle pair is given by $d(x_2 - x_1)/dt = T_L(dU/dz)(z_2 - z_1)$, where U is the mean streamwise velocity. Then, the structure function is given by Durbin's (1980) formula:

$$R(\Delta) = \left[\frac{\Omega^2}{L^2 + \Omega^2} \right]^{\frac{1}{3}} \left[\frac{\Omega^2}{\eta^2/\phi^3 + \Omega^2} \right]^{\frac{2}{3}} \left[1 + \frac{L^2 \Delta_x^2}{\Omega^2(\Omega^2 + L^2)} \right], \tag{14b}$$

where

$$\Delta_x = (x_2 - x_1)/\sqrt{2} \text{ and } \Omega^2 = \Delta^2 + \Delta_x^2.$$

From (10)–(13) the finite-difference equations can be obtained;

$$U_{m+1}^{(i)} = \{1 - \Delta T/T_L(m\Delta T)\} U_m^{(i)} + \sigma_w \left[\frac{2\Delta T}{T_L(m\Delta T)} - \frac{\Delta T^2}{T_L^2(m\Delta T)} \right]^{\frac{1}{2}} \xi_m^{(i)}, \tag{15}$$

$$z_{m+1}^{(1)} = z_m^{(1)} + \{\Delta T/2\sqrt{2}\} \{ \alpha_m [U_m^{(1)} + U_m^{(2)} + U_{m+1}^{(1)} + U_{m+1}^{(2)}] + \beta_m [U_m^{(1)} - U_m^{(2)} + U_{m+1}^{(1)} - U_{m+1}^{(2)}] \} + \kappa^{\frac{1}{2}} \{ \chi_m^{(1)} + \chi_m^{(2)} \} \{\Delta T\}^{\frac{1}{2}}, \tag{16}$$

$$z_{m+1}^{(2)} = z_m^{(2)} + \{\Delta T/2\sqrt{2}\} \{ \alpha_m [U_m^{(1)} - U_m^{(2)} + U_{m+1}^{(1)} - U_{m+1}^{(2)}] + \beta_m [U_m^{(1)} + U_m^{(2)} + U_{m+1}^{(1)} + U_{m+1}^{(2)}] \} + \kappa^{\frac{1}{2}} \{ \chi_m^{(1)} - \chi_m^{(2)} \} \{\Delta T\}^{\frac{1}{2}}, \tag{17}$$

where ξ_m and χ_m are sets of independent standard Gaussian random variables, ΔT is the small-time interval (in this study, $\Delta T/T_L = 0.05$) and α_m and β_m are defined by

$$\alpha_m = [1 + [2R(\Delta_m) - R^2(\Delta_m)]^{\frac{1}{2}}]/\sqrt{2} \tag{18}$$

$$\beta = (1 - \alpha_m^2)^{\frac{1}{2}}. \tag{19}$$

Here, the separation Δ_m is given by $(z_m^{(1)} - z_m^{(2)})/\sqrt{2}$. Numerical solutions of (15)–(17) lead to the final positions $z^{(1)}(t)$ and $z^{(2)}(t)$ of the two particles at a time t . One can determine the concentrations of the two particles for the n th particle pair from their positions, together with initial concentration distributions, using the concept of reversed dispersion.

In the case of reacting flows, however, we have to consider the effect of the concentration change (reaction) of a marked particle, because a marked particle reacts with another marked particle if two turbulent fluid elements with marked particles start from different concentration-species sources. The reaction is assumed to begin within the smallest turbulent eddy scale η at the interface, as shown by the

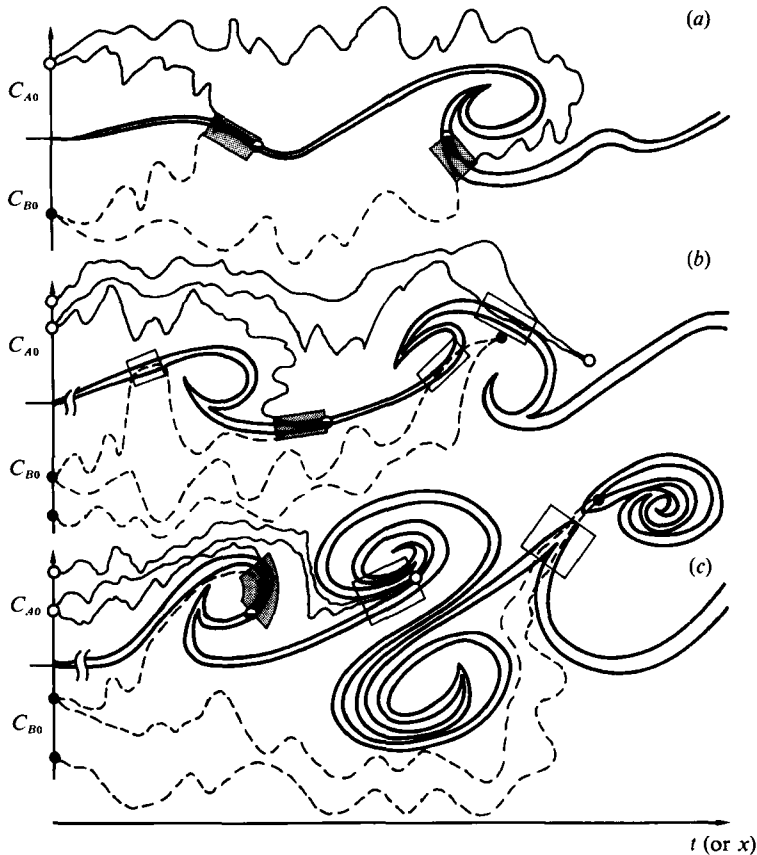


FIGURE 1. 1. Illustration of how marked particles of reactants mix together in different regions along the interface: (a) mixing mainly between pure A and B fluid particles; (b) mixing involving secondary mixing still at a simple interface; (c) mixing at multiply connected (or cutoff) interfaces. The light-dotted regions indicate where reaction is considered to take place in the present model, the dark-dotted region where reaction is not considered to take place. The reaction is assumed to begin only when the distance between a pair of A and B species becomes less than the Kolmogorov scale η . Solid and dotted lines show the trajectories of marked particles A and B respectively.

dark-dotted region in figure 1(a) illustrating the concentration change of marked particles in a non-premixed flow with two chemical reactants, A and B . Of course the marked particle A (or B) may mix and react with fluid of the other species in the interfacial region, before 'meeting' the particle B (or A) and reacting with it at a point (z, t) as shown by the light-dotted region in figure 1(b). In principle, for each time step between 0 and t these additional events should be considered. However, there may be a small probability that the particles remain close to the interface as in the light-dotted region of figure 1(b). Further, over the typical time for the mixing and reaction processes in the region under consideration (where $t/T_L < 10$), the flow visualization shows that most of the reaction front between A and B is convoluted but remains. However, a small part of the interface consists of 'cut-off' (or multiply connected) surfaces, caused by pinching-off of bulges in the interface as illustrated in figure 1(c) (the light-dotted region). The photographs show that these are indeed only small regions when $t/T_L < 10$ (figures 7 and 14) but become increasingly significant when $t/T_L > 10$.

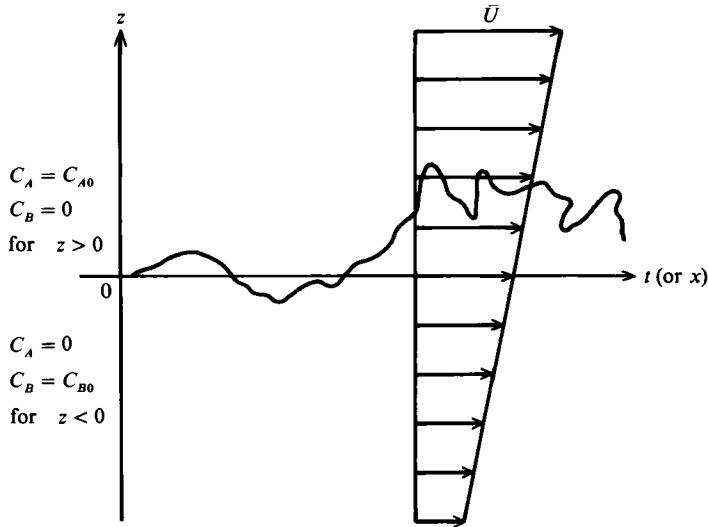


FIGURE 2. Illustration of a flow configuration and an initial concentration profile used for numerical calculations.

Therefore most of the fluid elements reaching any point (z, t) may be considered as coming from the unmixed reservoirs of species A and B without having reacted with the particles in the ambient fluid elements, and the reaction in the light-dotted region of figure 1 (c) is estimated to be rather small. Of course when the interface completely disintegrates so that there are significant numbers of patches of A mixed with B in the regions above and below the interface too far from the source or when high shear causes many patches, then our model will be no longer valid. For these physical reasons it is likely that this model *underestimates* the amount of reaction that has taken place by time t and is *applicable only* to a reacting zone not too far from the source and without high shear (though the limits of t/T_L and shear cannot be explicitly determined). Thus, we assume that when the distance between two marked particles of different species becomes less than the Kolmogorov scale η , i.e. $|z_1 - z_2| \leq \eta$, the reaction begins between the fluid elements A and B at the same rates as under well-mixed conditions. The reaction is assumed to continue until the particular meeting of two marked particles at (z, t) . This represents the effect on the reaction of the micromixing at scales less than η . Then, the concentration change of a marked particle i consisting of many molecules is given by the chemical law

$$\frac{dC_{i(n)}^{(1)}(z, t)}{dt} = \frac{dC_{j(n)}^{(2)}(z, t)}{dt} = -kC_{i(n)}^{(1)}(z, t)C_{j(n)}^{(2)}(z, t)[1 - \delta_{ij}], \quad (20)$$

where $C_{i(n)}^{(1)}(z, t)$ is the concentration of a marked particle 1 of the chemical species i for the n th particle pair, $C_{j(n)}^{(2)}$ the concentration of another marked particle 2 of the species j which meets the marked particle 1 at z and t , and δ_{ij} is the Kronecker delta.

The basis of the present model for combining the chemical reaction and mixing is that it is assumed, first, that the reaction rate constant k is either moderately fast or even slow, so that the chemical species are well mixed within the smallest scale of turbulent mixing. Consequently, (20) is used to combine the Lagrangian two-particle theory with the continuous chemical law, and therefore it may prevent the application of the present model to fast chemistry. To model turbulent mixing and

reaction with fast chemistry, quite different Lagrangian models are needed, such as that developed by Durbin (1989).

The integration of (20) along the particle trajectory gives the final concentration of a marked particle i for the n th particle pair:

$$C_{i(n)}^{(i)}(z, t) = C_{i(n)}^{*(i)}(z, t) - k \int_0^{t^*} C_{A(n)}^{(1)} C_{B(n)}^{(2)}(z, t') dt'. \quad (21)$$

Here, $C_{i(n)}^{*(i)}(z, t)$ is the concentration of a marked particle i for the n th particle pair at z and t which can be obtained by solving (15)–(17), and t^* is the time required for the two marked particles to travel from positions z_1 and z_2 satisfying $|z_1 - z_2| = \eta$ to a final meeting position z . If $C_{i(n)}^{(i)}(z, t)$ becomes negative, it is, of course, set to zero. Thus, the ensemble average for N -pairs (in this study $N = 1000$) gives concentration statistics in a non-premixed flow with a second-order reaction between two chemical species A and B

$$\overline{C_A(z, t)} = \frac{1}{2N} \sum_{n=1}^N [C_{A(n)}^{(1)} + C_{A(n)}^{(2)}], \quad (22a)$$

$$\overline{C_B(z, t)} = \frac{1}{2N} \sum_{n=1}^N [C_{B(n)}^{(1)} + C_{B(n)}^{(2)}], \quad (22b)$$

$$\overline{C_A C_A(z, t)} = \frac{1}{N} \sum_{n=1}^N [C_{A(n)}^{(1)} C_{A(n)}^{(2)}], \quad (23a)$$

$$\overline{C_B C_B(z, t)} = \frac{1}{N} \sum_{n=1}^N [C_{B(n)}^{(1)} C_{B(n)}^{(2)}], \quad (23b)$$

$$\overline{C_A C_B(z, t)} = \frac{1}{2N} \sum_{n=1}^N [C_{A(n)}^{(1)} C_{B(n)}^{(2)} + C_{B(n)}^{(1)} C_{A(n)}^{(2)}], \quad (24)$$

$$\overline{c_A c_A(z, t)} = \overline{C_A C_A(z, t)} - \overline{C_A(z, t)} \overline{C_A(z, t)}, \quad (25a)$$

$$\overline{c_B c_B(z, t)} = \overline{C_B C_B(z, t)} - \overline{C_B(z, t)} \overline{C_B(z, t)}, \quad (25b)$$

$$\overline{c_A c_B(z, t)} = \overline{C_A C_B(z, t)} - \overline{C_A(z, t)} \overline{C_B(z, t)}, \quad (26)$$

The values of $N = 1000$ and $\Delta T = 0.05 T_L$ used here were found to be sufficient to obtain results repeatable to within 10%. Here it should be noted that (22a) also shows the limitations of the prediction of the mean concentration of the reactant in a region too far from the source or in high shear turbulence. When the reactants are stoichiometrically mixed and reacting, the mean concentration of the reactants must approach zero at infinite mixing time under any mixing conditions. However, the present model cannot statistically predict mean concentration (normalized by the initial concentration) of less than 0.25. This is because in the present model the marked particle only reacts with the other marked particle coming from the source region ($x = 0$), while reactions with the ambient fluid elements are assumed to be negligible over the timescale of interest.

3.2. Flow and concentration fields for model computations

As mentioned above, the present model can only treat a simple homogeneous flow over the cross-sectional plane. Therefore, we considered the simplest non-premixed reacting flow with an initial concentration profile of a mixing-layer type and a uniform mean shear, as shown in figure 2, and discussed the segregation parameter α only on the averaged interface between fluids A and B , i.e. on the plane $z = 0$ in the

figure. The effect of inhomogeneity on α was small, and initial concentration profiles did not affect α much on the averaged interface ($z = 0$), except in the region near the source. Also, α and the correlation coefficient of concentration fluctuations were not affected much by the transverse coordinate z , except in the outer edge region of the mixing layer. Of course, other quantities such as the mean concentration and intensity of concentration fluctuation strongly depend on the transverse coordinate. If required, their transverse profiles can also be computed by the present model.

To investigate the effect of some parameters on the concentration correlation, the computations in §4.2 were mainly done for grid-generated turbulence. Experimental properties of the flow field used in (13) and (14) of the present stochastic model were taken to be the measured values of $x/M = 5$ in the empirical formula obtained in grid-generated turbulence by Komori *et al.* (1989) which will be introduced in §4.4:

$$\sigma_w(x) = [0.071(x/M)^{-1.5}]^{\frac{1}{2}} U, \quad (27)$$

$$L(x) = 0.075M(x/M)^{0.49}, \quad (28)$$

$$\epsilon(x) = \sigma_w^3(x)/L(x), \quad (29)$$

An estimate of $T_L(x/M = 5)$ is $L(x)/\sigma_w(x)$, (30)

but in turbulence decaying as fast as this, this is not a reliable estimate of the 'turnover time'. Here M and U are the grid mesh size and mean velocity of the flow. The above formula is very close to the measurements by Stapountzis *et al.* (1986). The effect of the mean shear was studied by changing the values of non-dimensional shear τ , defined by $(dU/dz)T_L$. For comparisons with the previous measurements (§4.4), the experimental properties of the model and the mean shear were given by the measured values in each experiment.

4. Results and discussion

4.1. Dimensionless groups in turbulent reacting flows

In an inhomogeneous turbulent reacting flow the full equation for the concentration of one species C_A is given by (3a). To determine the key scaling parameters we have to consider three effects with different time- and space scales. By considering the straining motion on the smallest scales (Batchelor 1952), it follows that in a turbulent flow the smallest lengthscale for the concentration field is $\iota_c \approx (\nu^3/\epsilon)^{\frac{1}{2}} Sc^{-\frac{1}{2}}$, where the Schmidt number $Sc = \nu/\kappa$. For estimating the effect of reactions we need to estimate the smallest timescale of the concentration field, which is of the same order as that of the smallest fluid motions, namely $(\nu/\epsilon)^{\frac{1}{2}} \approx T_L Re_t^{-\frac{1}{2}}$ where $Re_t = u'L/\nu$ is the turbulent Reynolds number based on the integral scale. Therefore a measure of the effect of the rate of reaction on the smallest concentration gradients of C_A and C_B across an interface is the ratio of this timescale to that of the reaction rate $[k(C_A C_B)^{\frac{1}{2}}]^{-1}$, i.e. the Damköhler number for the microscale motions

$$Da_{\text{Kol}} = (\nu/\epsilon)^{\frac{1}{2}} k(C_A C_B)^{\frac{1}{2}} \quad (31)$$

(Gibson & Libby 1972). If $C_A C_B$ is represented by the initial concentrations, Da_{Kol} may be given by

$$Da_{\text{Kol}} = (\nu/\epsilon)^{\frac{1}{2}} k(C_{A0} C_{B0})^{\frac{1}{2}}. \quad (32)$$

If $Da_{\text{Kol}} \gg 1$, then the reaction occurs faster than the time for the smallest eddies to feed the interface layer with the species A and B . This results in C_A tending to zero on B 's side of the interface and vice versa. This kind of reaction-diffusion layer occurs in flames but not in more slowly reacting chemical engineering or atmospheric

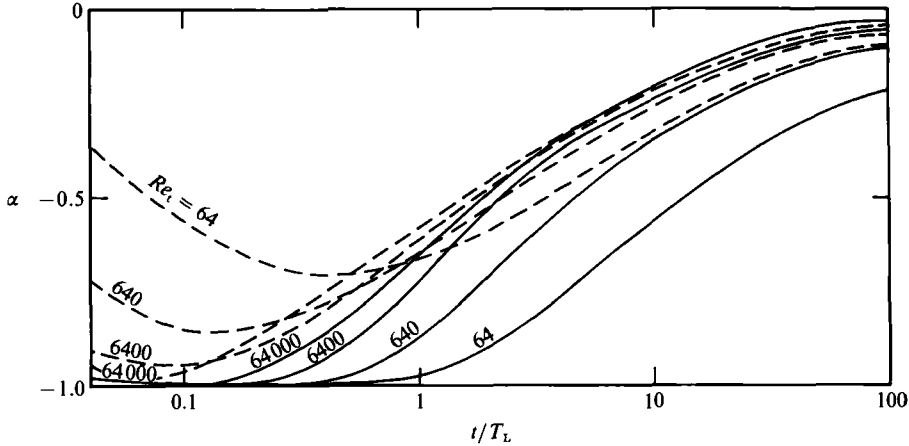


FIGURE 3. Effects of the turbulent Reynolds number Re_t on the segregation parameters α under non-reactive conditions: —, $Sc = 600$; ---, $Sc = 1$.

chemistry problems where the timescale of the reaction is more comparable with the integral scale of the turbulent motions T_L . For a moderately fast or slow reaction, an integral-scale Damköhler number is defined by

$$Da_I = T_L k(C_{A0} C_{B0})^{\frac{1}{2}}, \quad (33)$$

and it is related to Da_{Kol} by

$$Da_I = Da_{Kol} Re_t^{\frac{1}{2}}. \quad (34)$$

Significant changes in the development of the reaction are found when Da_I is of order 1. If $Da_{Kol} \ll 1$, the micromixing is the same as for a non-reacting scalar, but wherever this mixing has occurred there is slow decay of C_A and C_B .

Thus the key dimensionless parameters for a turbulent mixing process with reactions are Re_t , Sc and Da_I or Da_{Kol} .

4.2. Effects of varying the turbulent Reynolds, Schmidt and Damköhler numbers and the mean shear on the concentration correlations

In order to investigate the effect of the turbulent Reynolds number Re_t , based on the integral scale, on the segregation parameter α , calculations of α on the averaged interface of $z = 0$ were first conducted by changing Re_t , i.e. σ_w in (27). The results for two non-reacting cases with the Schmidt numbers of 1 and 600 and without mean shear are shown in figure 3. The effect of the turbulent Reynolds number Re_t on α is significant but its effect becomes small in the mixing region of $t/T_L > 1$ with increasing Re_t . The effect of the Schmidt number Sc is obvious in the initial mixing region of $t/T_L < 1$, but it also becomes small at a very high Re_t . These results are consistent with the effects of molecular motions becoming small with increasing Re_t .

For reactive cases without shear, α was calculated by changing Re_t with the Damköhler number Da_{Kol} held constant. Figures 4 and 5 show the distributions of α for $Da_{Kol} = 0.05$ and 0.5 , respectively. The distributions tend to converge to a quite different curve between the two Schmidt numbers with increasing time of mixing, but α still depends on Re_t . In particular, its dependency on Re_t is significant for $Sc = 1$ and $Da_{Kol} = 0.5$. Thus the segregation parameter α cannot be uniquely determined by Da_{Kol} , and therefore we have to seek to understand other effects on α by fixing the turbulent Reynolds number Re_t to a constant value. For further calculations in this section, Re_t is set to 64 (cf. Komori *et al.* 1989), which is at the

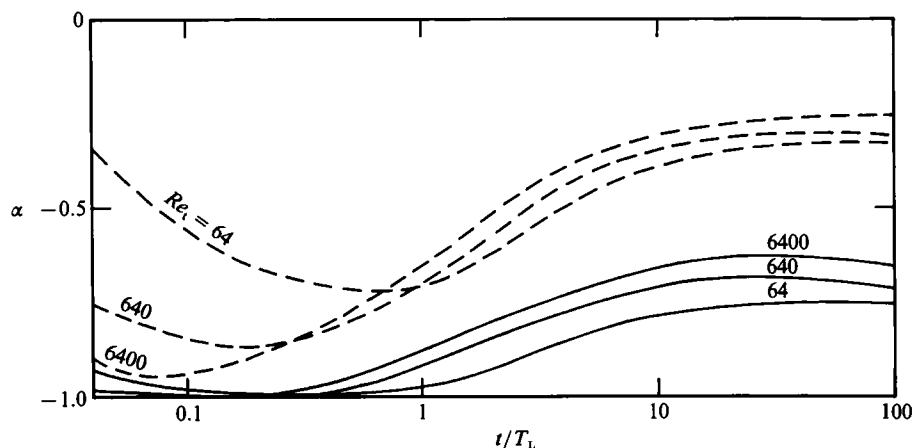


FIGURE 4. Time variations of the segregation parameter α for different values of the turbulent Reynolds number Re_t under reactive conditions with a constant Damköhler number of $Da_{kol} = 0.05$: —, $Sc = 600$; ---, $Sc = 1$.

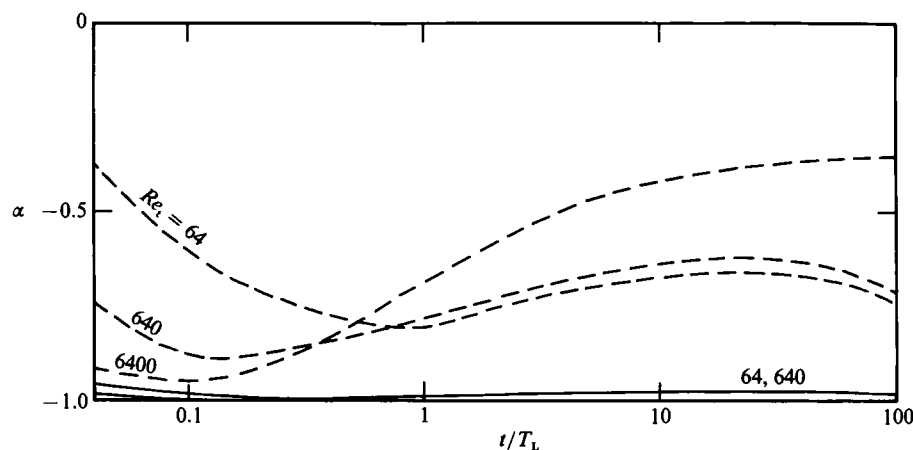


FIGURE 5. Time variations of the segregation parameter α for different values of the turbulent Reynolds number Re_t under reactive conditions with a constant Damköhler number of $Da_{kol} = 0.5$: —, $Sc = 600$; ---, $Sc = 1$.

same order as in other laboratory experiments in grid-generated turbulent flows and in most direct simulations of reacting flows.

Figure 6 shows the variations of α in flow without shear versus the integral-scale Damköhler number Da_I . For a non-reactive case ($Da_I = 0$), α grows from a negative value to zero with the relative time of mixing t/T_L . As the turbulent Reynolds number of 64, is rather low, the effect of the Schmidt number is very large in the initial mixing region, as seen in figure 3. However, when both Re_t and Sc are set to constant values, α is uniquely determined by Da_I for the specific condition of $C_{A0}/C_{B0} = 1$. Da_I has a marked effect on α in the mixing region of $t/T_L > 1$, where α decreases with increasing Da_I . For a faster chemical reaction, α approaches -1 . This means that the chemical reaction is so fast that the interfacial part where A coexists with B becomes narrow. At the same time outside the interfacial region the chemical product spreads by molecular and turbulent diffusion. The chemical product within

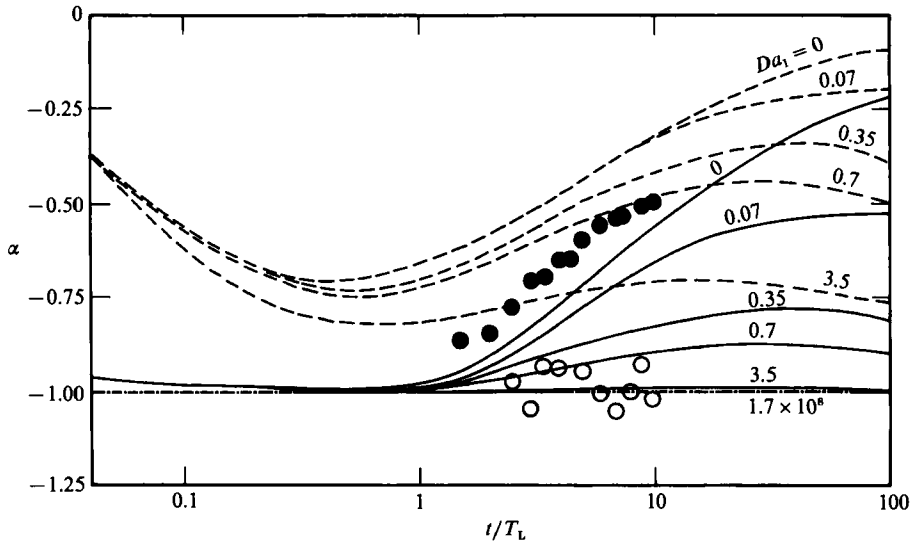


FIGURE 6. Time variations of the segregation parameter α for different values of the Damköhler number Da_1 : —, $Sc = 600$, $\beta = 1$; ---, $Sc = 1$, $\beta = 1$; - - - -, prediction for the reacting flow of Komori *et al.* (1991*a*) ($Da_1 = 1.7 \times 10^8$); ●, measurements of Komori *et al.* (1989) in a non-reacting flow; ○, measurements of Komori *et al.* (1991*a*) in a reacting flow ($Da_1 = 1.7 \times 10^8$).

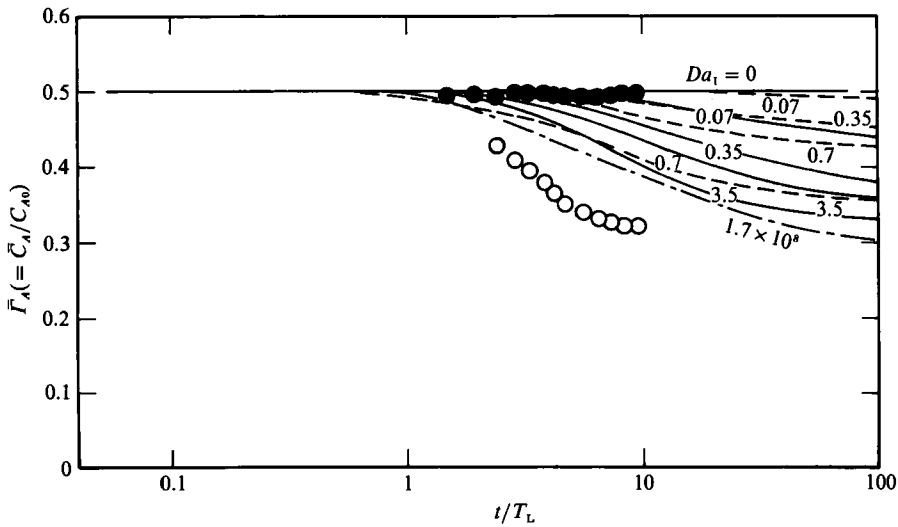


FIGURE 8. Time variations of the normalized mean concentration $\bar{F}_A (= \bar{C}_A / C_{A0})$ for different values of the Damköhler number Da_1 : —, $Sc = 600$, $\beta = 1$; ---, $Sc = 1$, $\beta = 1$; - - - -, prediction of Komori *et al.* (1991*a*) for a reacting flow ($Da_1 = 1.7 \times 10^8$); ●, measurements of Komori *et al.* (1989) in a non-reacting flow; ○, measurements of Komori *et al.* (1991*a*) in a reacting flow ($Da_1 = 1.7 \times 10^8$).

the reacting turbulent interfacial region can be clearly seen as the bright streaks in the photographs of figure 7 (plate 1). The photograph is of Komori, Kanzaki & Murakami (1991*a*) two-dimensional shear-free grid-generated turbulence for a reaction between hydrochloric acid and sodium hydroxide using a laser-induced fluorescence technique at $x/M = 2-20$. For the largest value of Da_1 , 3.5, the mean

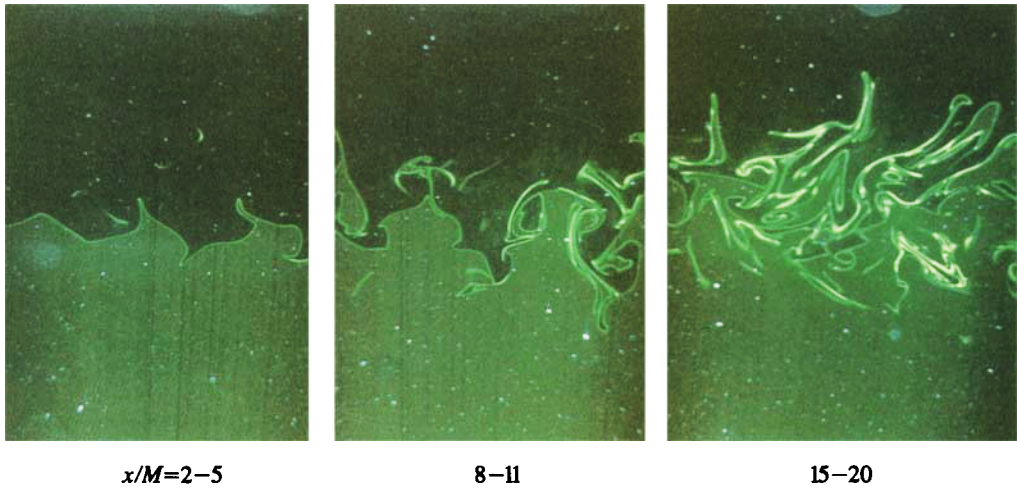


FIGURE 7. Photographs from Komori *et al.* (1991a) of the chemical product visualized by a laser-induced fluorescence technique at $x/M=2-20$ ($t/T_L=1-10$) for two-dimensional shear-free layer in grid-generated turbulence with the reaction between hydrochloric acid and sodium hydroxide. The half-thickness of the product layer is illuminated by the fluorescence. Most of the isolated blobs of product in the photographs are generated not by the disintegration of the interface but by the spanwise contortion of the three-dimensional continuous interface, since the thin laser sheet is in the vertical direction.

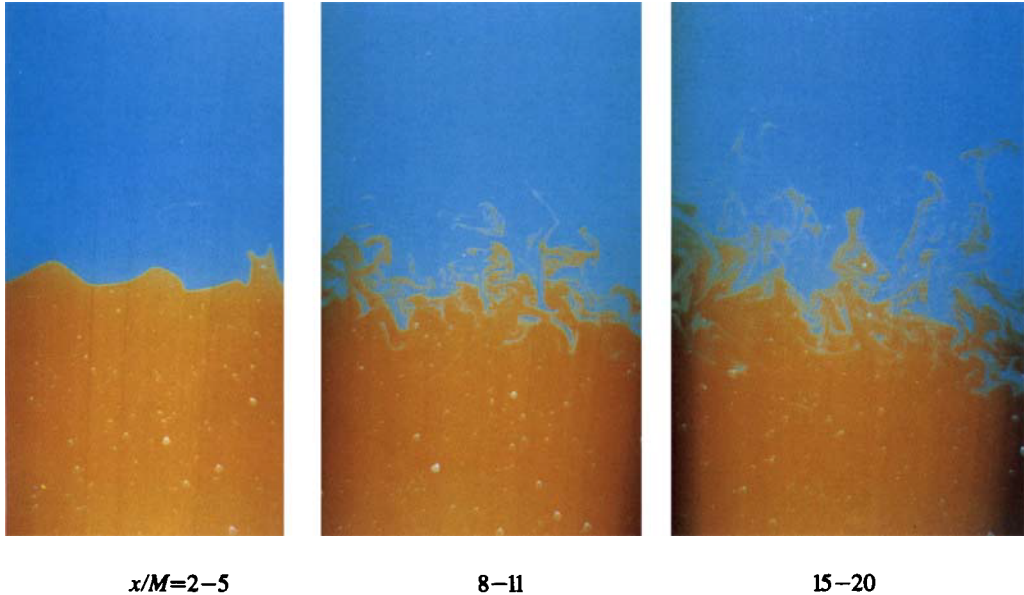


FIGURE 14. Photographs from Komori *et al.* (1989) of the motions of the interface visualized by a combined laser-induced fluorescence and laser-scattering technique at $x/M=2-20$ ($t/T_L=1-10$) for two-dimensional shear-free layer in grid-generated turbulence without reaction. Most of the isolated blobs are due to the spanwise contortion of the continuous interface, as mentioned in figure 7.

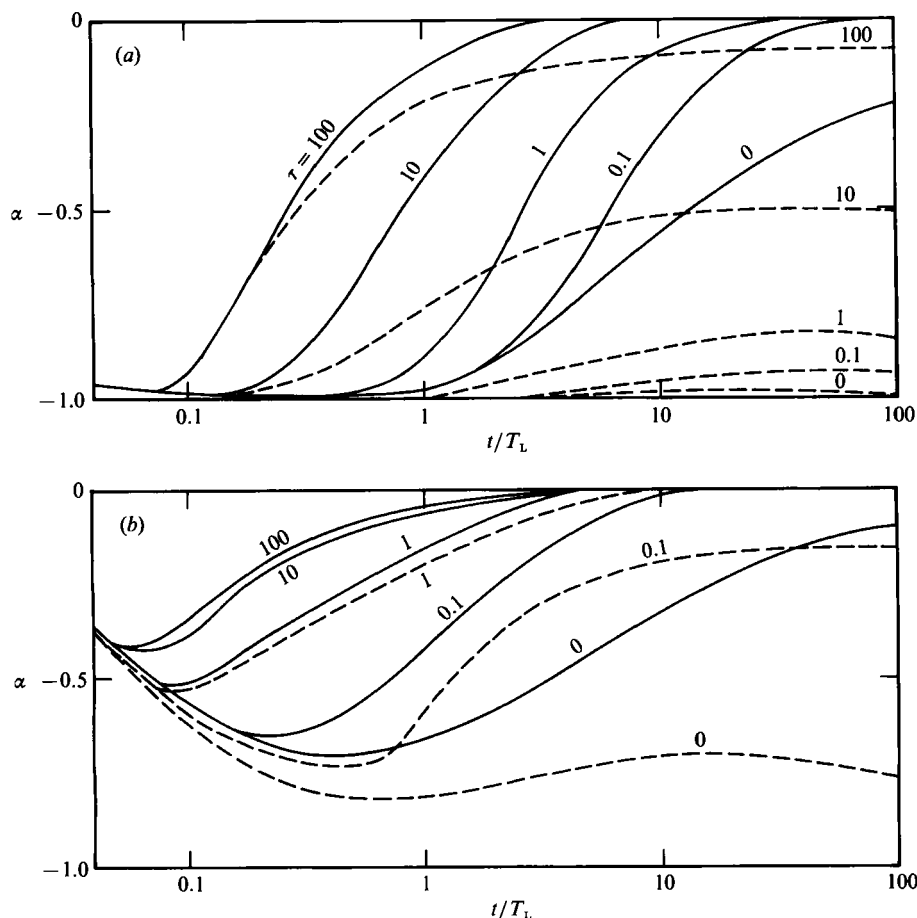


FIGURE 9. Time variations of the segregation parameter α for different values of the dimensionless mean shear τ : (a) at a high Schmidt number of $Sc = 600$; (b) at a low Schmidt number of $Sc = 1$: —, $Da_1 = 0$ (without reaction), $\beta = 1$; ---, $Da_1 = 3.5$ (with reaction), $\beta = 1$.

reaction rate approached the maximum at $t/T_L \sim 5$ and then decreased with increasing t/T_L , because of the rapidly generated chemical product. This results in the slow decrease of the mean concentration in the mixing region of $t/T_L \gtrsim 20$, as shown in figure 8. This behaviour is in qualitative agreement with the measurements of Komori *et al.* (1991 *a*) in decaying turbulence with a rapid reaction between acetic acid and ammonium hydroxide (see §4.4), though this comparison may be beyond the application limit of the present model. A physical explanation of these variations of α with the mixing time will be given in §4.3.2.

To promote the chemical reaction in a flow with a fast reaction, the turbulent motion has to distort or stretch the interface layer occupied by the chemical product and to promote the turbulent and molecular mixing between *A* and *B*. High shear is expected to aid this process. Certainly, the effect of the shear is likely to promote the mean chemical reaction rate, significantly as shown in figure (9*a, b*) by the increase of α with dimensionless mean shear $\tau [= T_L (dU/dz)]$. This is consistent with the effect of shear to increase mixing and the rate of decay of scalar fluctuations (Durbin 1980; Stapountzis & Britter 1989). Note that we do not consider that the present model can fully be applied to flows with high shear.

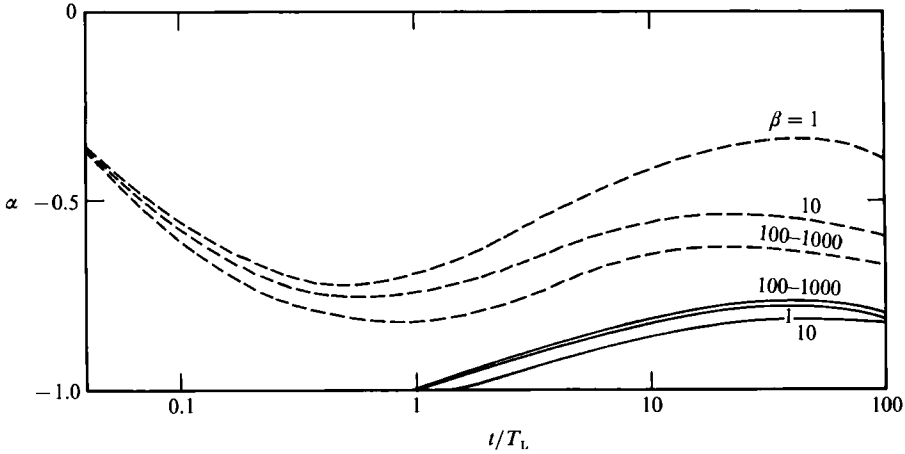


FIGURE 10. Time variations of the segregation parameter α for different values of the ratio of the initial concentrations β in reactive conditions: —, $Sc = 600$, $Da_1 = 0.35$; ---, $Sc = 1$, $Da_1 = 0.35$.

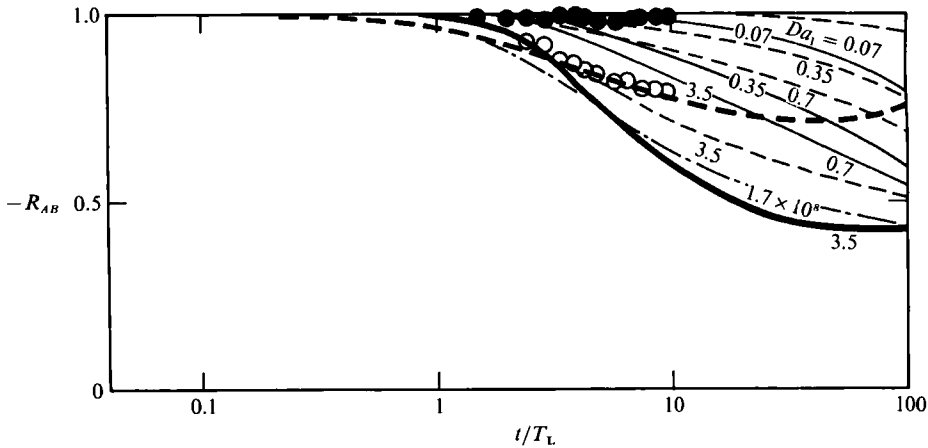


FIGURE 11. Time variations of the correlation coefficient between the concentration fluctuations R_{AB} for different values of the Damköhler number Da_1 and mean shear τ : —, $Sc = 600$, $\beta = 1$; ---, $Sc = 1$, $\beta = 1$; — · —, prediction of Komori *et al.* (1991a) for a reacting flow ($Da_1 = 1.7 \times 10^8$); ●, measurements of Komori *et al.* (1989) in a non-reacting flow; ○, measurements of Komori *et al.* (1991) in a reacting flow ($Da_1 = 1.7 \times 10^8$). The heavy lines show the case with the dimensionless mean shear $\tau = 0.1$.

Thus, when Re_t , Sc and τ are given, the segregation parameter α is uniquely determined by Da_1 . However, the ratio of the initial concentrations $\beta (= C_{A0}/C_{B0})$ also significantly affects α , as shown in figure 10 for the case $Sc = 1$. This shows that when we estimate α in a reacting flow we have to consider the effect of β in addition to the effects of Da_1 , Re_t , Sc and τ .

For reference the variation of the correlation coefficient $R_{AB} (= \overline{c_A c_B} / c'_A c'_B)$ between concentration fluctuations c_A and c_B against the Damköhler number Da_1 is shown in figure 11. The coefficient R_{AB} is always equal to -1 in non-reactive conditions since $c_A = -c_B$. However, the correlation decays to zero in reactive

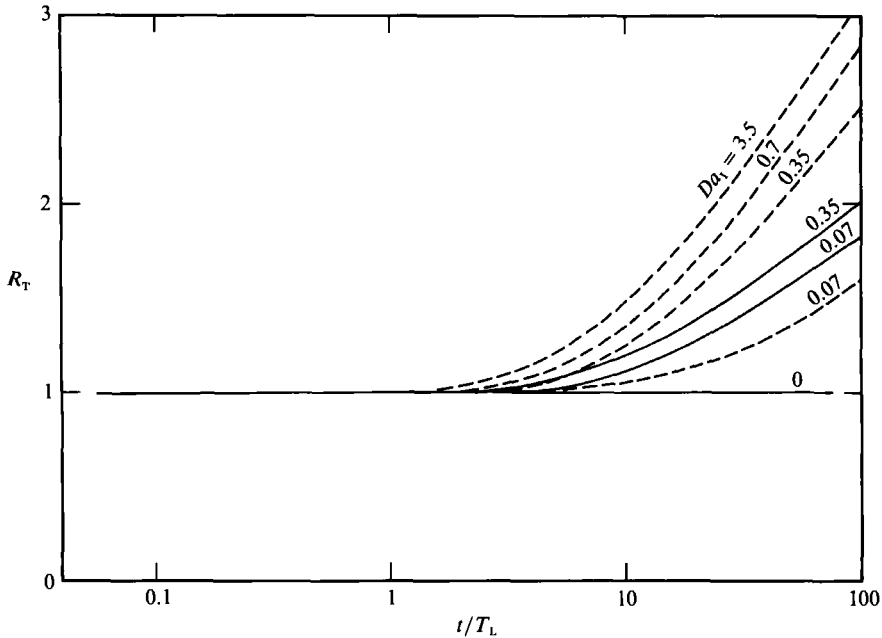


FIGURE 12. Time variations of the ratio R_T of the concentration correlation with reaction to the mean-squared value of one-species concentration fluctuation without reaction with the Damköhler number Da_1 : —, $Sc = 600$, $\beta = 1$; ---, $Sc = 1$, $\beta = 1$.

conditions with increasing Da_1 . The behaviour of R_{AB} is in qualitative agreement with the recent measurements of Komori *et al.* (1990) and SaeTRAN *et al.* (1989) in a reacting mixing layer in grid turbulence. This decaying correlation is easily understood from a consideration of the chemical product. As the shear helps to sweep away the product from the interface layer between A and B fluids, it decreases the correlation coefficient $-R_{AB}$, as shown by heavy lines for $\tau = 0.1$ and $Da_1 = 3.5$.

In order to confirm the Toor's (1969) hypothesis the dimensionless ratio of the concentration correlation $\overline{c_A c_B}$ with reaction to the mean-squared value of the concentration fluctuation c_A^* without reaction, $R_T = \overline{c_A c_B} / c_A^{*2}$ was calculated and was normalized by the ratio at $t/T_L = 0.05$ (see figure 12). Toor's hypothesis is that $R_T = 1$. The predictions are in good agreement with the hypothesis only for the initial mixing period when $t/T_L \lesssim 1$. For mixing over a larger period when $t/T_L \gtrsim 1$, the discrepancy between the predictions and the hypothesis becomes larger as Da_1 increases. This suggests that the Toor's hypothesis is only valid in the initial mixing region and in very slow reactions (though the present model is also flawed for longer periods of mixing and for the case of fast chemistry).

4.3. Limits on the segregation parameter α and a physical explanation for the variations of α with the mixing time

4.3.1. Limits on the segregation parameter α

In §4.2, the segregation parameter α ranged from -1 to 0 . Here we consider the physical limits of α . In the absence of molecular diffusion A molecules cannot coexist with B molecules and so the reaction does not proceed. Therefore in a non-premixed flow where no fluid elements contain both A and B initially, i.e. $\overline{C_A C_B} = 0$ at $t = 0$

for all z , there can be no subsequent correlation between A and B , i.e. $\overline{C_A C_B} = 0$. But since $\overline{C_A} \neq 0$, $\overline{C_B} \neq 0$,

$$\alpha = -1 + \overline{C_A C_B} / \overline{C_A} \overline{C_B} = -1 \quad \text{for } t > 0. \quad (35)$$

With molecular diffusion in a turbulent flow mixing leads to $\overline{C_A C_B}$ increasing, but $\overline{c_A c_B}$ has a limit which can be derived from the mass balance equation. In the absence of reaction, two concentrations normalized by the initial concentrations Γ_A^* ($= C_A^*/C_{A0}$) and Γ_B^* ($= C_B^*/C_{B0}$) satisfies

$$\Gamma_A^* + \Gamma_B^* = 1. \quad (36)$$

For the respective time-averaged and fluctuating concentrations,

$$\overline{\Gamma_A^*} + \overline{\Gamma_B^*} = 1, \quad (37)$$

and

$$\gamma_A^* = -\gamma_B^*. \quad (38)$$

The segregation parameter α is given by

$$\alpha = \overline{\Gamma_A^* \Gamma_B^*} / [\overline{\Gamma_A^*} \overline{\Gamma_B^*}] - 1 = -\overline{\gamma_A^{*2}} / [\overline{\Gamma_A^*} (1 - \overline{\Gamma_A^*})]. \quad (39)$$

Since $0 \leq \Gamma_A^* \leq 1$ and $0 \leq \Gamma_B^* \leq 1$ everywhere in the flow domain, it follows that $0 \leq \overline{\Gamma_A^*} (1 - \overline{\Gamma_A^*}) \leq \frac{1}{4}$ and $\overline{\Gamma_A^* \Gamma_B^*} \geq 0$. Therefore, we obtain a limit for α in a non-premixed non-reacting flow

$$-1 \leq \alpha \leq 0. \quad (40)$$

On the centreline, $z = 0$, (see figure 2) both $\overline{\Gamma_A^*}$ and $\overline{\Gamma_B^*}$ are equal to $\frac{1}{2}$, and then (39) leads to $\alpha = -4\sigma_c^2$, where σ_c^2 is the variance of the concentration fluctuation ($= \overline{\gamma_A^{*2}} = \overline{\gamma_B^{*2}}$). On the other hand, the mixing and reaction is assumed in (20) to be confined to a thin interface. Initially, for say $t/T_L \lesssim 0.5$, the interface is sharp and is not convoluted. Then the form of the fluctuating signal of concentration at a point on the centreline is approximately a rectangular wave form. In that case $\sigma_c^2 \sim \frac{1}{4}$, and (39) implies that $\alpha \sim -1$. However, downstream where $t/T_L \sim 1$, the experimental photographs in figures 7 and 14 show that the interface becomes convoluted, but still singly convoluted. There A and B are separated by many thin layers with the same order of thickness as the molecular diffusion layer (as will be shown in (45) and (46)). Therefore the concentration profiles of A and B vary smoothly across these layers and may be approximated by sine curves. In that case $\sigma_c^2 \sim \frac{1}{8}$ and $\alpha \sim -0.5$. This is about the maximum values of α that can be expected in the range of t/T_L for which the present model is valid (this point was made by a referee).

In the presence of a second-order chemical reaction, by subtracting (3b) from (3a) or by considering the mass-conservation equations for A and B species with the same molecular diffusivity, we show how these two concentration fields are related to their values without any reaction, namely

$$\Gamma_A^* - \Gamma_B^* = \Gamma_A - \Gamma_B, \quad (41)$$

where Γ_A^* and Γ_B^* are the normalized concentrations of A and B without reaction and Γ_A and Γ_B are the normalized concentrations of A and B with reaction. Here the initial concentrations C_{A0} and C_{B0} are used for the normalization and they are assumed to have the same value, $C_{A0} = C_{B0}$. From (36) together with (41), we derive α with reaction in terms of the mean and fluctuating concentration values with and without reaction, namely

$$\begin{aligned} \alpha &= \overline{[\gamma_A(\gamma_A - \gamma_A^* + \gamma_B^*)]} / [\overline{\Gamma_A}(\overline{\Gamma_A} - \overline{\Gamma_A^*} + \overline{\Gamma_B^*})] \\ &= \overline{[\gamma_A(\gamma_A - 2\gamma_A^*)]} / [\overline{\Gamma_A}(\overline{\Gamma_A} + 1 - 2\overline{\Gamma_A^*})]. \end{aligned} \quad (42)$$

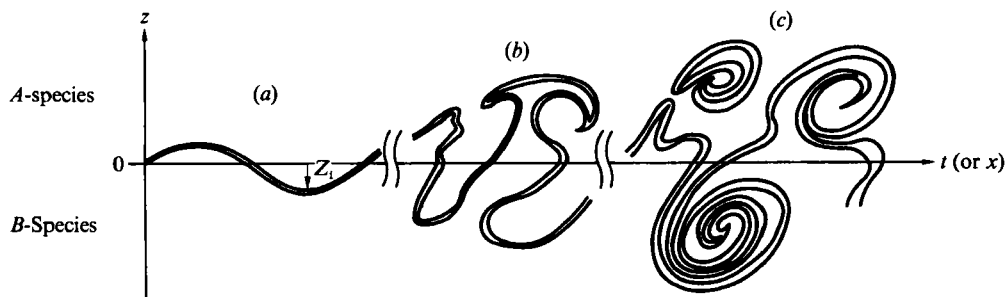


FIGURE 13. Sketch of the motions of the interface: (a) at small mixing time ($t/T_L \ll 1$); (b) at moderate mixing time ($t/T_L \sim 1$); (c) at large mixing time ($t/T_L \gg 1$).

Therefore measurements or simulations of the concentration A with and without reaction provide α in a non-premixed reacting flow. However, for most reacting flows there is a high probability that if $0 < \gamma_A < \gamma_A^*$, $\gamma_A > 0$ and that if $0 > \gamma_A > \gamma_A^*$, then $\gamma_A < 0$. From (42), this would result in negative values of α . Thus, even with a reaction occurring, α may satisfy the inequality (40). Of course in the extreme limit of $k \rightarrow \infty$ or ($Da_1 \rightarrow \infty$) $\Gamma_A \Gamma_B \rightarrow 0$ and therefore $\alpha \rightarrow -1$.

4.3.2. *A physical explanation for the variations of the segregation parameter α with the time of mixing*

As mentioned in §4.2, the predicted values of α increased from near -1 to zero with the mixing time and decreased with increasing Damköhler number Da_1 . In order to explain physically the behaviour of α , we consider an experiment where a uniform concentration C_{A0} , of A is introduced into a turbulent flow above a uniform concentration C_{B0} (see the concentration profile of a mixing-layer type shown in figure 2). The initial position of the interface is $z = 0$. We also consider the development of the mixing with time t or with distance x if A and B are introduced at the plane $t = 0$ (or $x = 0$) in a uniform flow. The interface is subsequently defined as the position Z_1 of fluid elements that start at $z = 0$ and at $t = 0$ (or $x = 0$), as shown in figure 13 (it does not define the molecules' position):

$$dZ_1/dt = w(Z_1, t). \tag{43}$$

Initially the interface flaps up and down and its contortions gradually grow with time. The motions of the interface can clearly be seen in the photographs (figure 14) (plate 1), visualized by combined laser-induced fluorescence and laser-scattering technique, in Komori *et al.*'s (1989) two-dimensional shear-free layer in grid-generated turbulence. Its r.m.s. displacement $Z'_1 \sim w't$, where w' is the r.m.s. value of w , and, if the large-scale turbulence is approximately Gaussian, the mean concentration profiles of A and B , C_A and C_B , have error function profiles, e.g.

$$C_A = \frac{1}{2}C_{A0} \{1 + \text{erf}[z/(\sqrt{2}\delta(t))]\}, \tag{44}$$

where $\delta = Z'_1 \sim w't$.

The mixing between A and B , and the correlation between C_A and C_B develops as molecular diffusion occurs across the interface. For a very short time, less than a Kolmogorov microscale $(\nu/\epsilon)^{\frac{1}{2}}$, the transfer would be controlled by molecular diffusion as described by

$$C_A \sim \frac{1}{2}C_{A0} \{1 + \text{erf}[(z - z_i(t))/\sqrt{2}\delta_i]\}, \tag{45}$$

where

$$\delta_i = (2\kappa t)^{\frac{1}{2}}.$$

At a time t (or distance x), the thickness of the interface layer δ is of the order of the spreading distance $\Delta(t)$ between two fluid elements starting close together at $t = 0$. At the instantaneous position of the interface, $C_A C_B \sim \frac{1}{4} C_{A0} C_{B0}$. But the time-average value of $C_A C_B$ depends on how long the interface layer is at the measuring point. This depends on how convoluted the interface has become. If there are N intersections between a plane $x = \text{constant}$ and the interface, the mean value of $C_A C_B$ will be proportional to the total cross-section per unit span intersected by the interface, divided by the vertical distance Z' over which the interface is dispersed. Therefore,

$$\overline{C_A C_B} \sim \sum_{i=1}^N \frac{\delta_i}{Z'} \frac{1}{4} C_{A0} C_{B0}. \quad (46)$$

In the presence of reaction the concentrations in the interface layer may decrease according to a decay factor

$$D = 1/(1 + \psi Da_1 t/T_L), \quad (47)$$

where ψ is a constant. Of course we here assume that the microscale mixing is unchanged by chemical reaction. Then,

$$\overline{C_A C_B} \sim \sum_{i=1}^N \frac{\delta_i}{Z'} D^2 \frac{1}{4} C_{A0} C_{B0}. \quad (48)$$

Since the volume fraction of the fluid occupied by only A or only B is much larger than that of the interface layer where both A and B exist (provided that the interface layer has not been significantly broken up), the product of the mean concentrations near $z = 0$ is given approximately by

$$\bar{C}_A \bar{C}_B = \frac{1}{4} C_{A0} C_{B0} \quad \text{for } t/T_L > 0 \quad \text{if } Da_{\text{Kol}} = 0. \quad (49)$$

The same result also holds for $t/T_L < 1$ and $Da_{\text{Kol}} < 1$. But when $Da_{\text{Kol}} > 1$ and $t/T_L > 1$, the interface becomes convoluted and the reaction can lead to large 'islands' of depleted C_A or C_B on each side of the interface over a scale δ . In that case on $Z = 0$, $C_A > \frac{1}{4} C_{A0}$ (a rough estimate between $\frac{1}{2}$ and 0) and $C_A C_B > \frac{1}{16} C_{A0} C_{B0}$. From (48) and (49) an estimate for α on $z = 0$, when $t/T_L < 1$, is

$$\alpha = -1 + D^2 \sum_{i=1}^N \frac{\delta_i}{Z'}. \quad (50)$$

For very small time when the interface is not convoluted, $\Delta \sim \epsilon^{\frac{1}{2}} t^{\frac{3}{2}} \sim w' t^{\frac{3}{2}} T_L^{-\frac{1}{2}}$ when $\eta \ll \Delta \ll L$. Then, since $Z' \sim w't$, it follows that α grows with time according to

$$\alpha = -1 + D^2 \lambda (t/T_L)^{\frac{1}{2}}, \quad (51)$$

where

$$\lambda = \delta/\Delta \quad \text{and} \quad \delta = \sum_{i=1}^N \delta_i.$$

Thus, when $Sc \sim 1$, we expect α to approach zero in time $t \sim T_L$, since $\Delta \sim \delta$. If $Sc \gg 1$, (e.g. for diffusion in liquids, where $Sc \sim 10^3$), α increases from -1 to 0 at a rate that is very much less (initially $O(Sc)^{-\frac{1}{2}}$ less) since $\Delta \gg \delta$. Then the growth of α is very slow, compared to that for $Sc \sim 1$.

In a reacting flow, the decay factor D in (47) becomes significant for a large mixing time when Da_1 is small, and therefore α beings to the decrease in the well-developed mixing region. These time variations of α which are expected from (51) are in qualitative agreement with the predictions by the present stochastic model (cf. figure

6). If Da_1 is large, the estimate in (47) and (50) for α is not valid. However, the model has the correct qualitative trend, namely that $\alpha \rightarrow -1$ as $Da_1 \rightarrow \infty$ (cf. Komori *et al.* 1990; Saetran *et al.* 1989 and Hill 1976).

4.4. Comparisons of the predictions to the new experiments

There have been no previous studies which have showed the time (or downstream) variations of the concentration statistics of two species being mixed in reacting or non-reacting shear-free turbulence. Recently, Komori *et al.* (1989) developed a combined laser-induced fluorescence and laser-scattering technique to measure simultaneously the instantaneous concentrations of two non-reacting species and showed the downstream variations of the concentration statistics in shear-free grid-generated turbulence without a reaction. Their test apparatus was a water tunnel with a square cross-section of 0.1×0.1 m and a turbulence-generation grid was installed at the entrance of the test section. Aqueous solutions of the species *A* and *B* were pumped up from two big storage tanks to the head tanks, and they passed through a contraction tunnel, which was separated by a thin splitter plate into two upper and lower sections set just in front of the turbulence-generation grid. The mesh size and the diameter of the rods were 0.02 m and 0.003 m, respectively. The mean velocities of the upper (species *A*) and lower (species *B*) streams were set to the same value of 0.25 m/s, so that the Reynolds number based on the mesh size was 5000. The turbulent Reynolds number estimated at $x/M = 5$ was 64. Rhodamine 610 and small latex particles of 0.1 μm were respectively used as species *A* and *B*, and each was homogeneously premixed in the upper and lower streams, respectively. When a high-power argon-ion laser is shot into the mixing region of the test section, laser fluorescence and the Mie-scattering light were obtained from species *A* and *B*, respectively. The two types of light were separated by optical filters and they were detected by the photomultipliers.

The mean concentrations of species *A*, the segregation parameter and the correlation coefficient between the concentration fluctuations, which were measured in non-reacting shear-free turbulence by Komori *et al.* (1989), are shown by solid circles in figures 6, 8 and 11. The measured segregation parameter α clearly shows an increase with relative time of mixing t/T_L and the measurements agree well with the predictions for $Da_1 = 0$ in the region $t/T_L < 10$. However, the measured α begins to deviate from the prediction in the region $t/T_L \sim 10$, and it tends to approach a constant value of about -0.5 with increasing t/T_L . This may be because the turbulence is decaying in the experiment, and so, the comparison between these measurements and the predictions may be limited to the region of $t/T_L < 10$. There the mean concentration, normalized by the initial concentration, and the correlation coefficient between the concentration fluctuations c_A and c_B are always equal to 0.5 and -1.0 on the central plane of the mixing region, respectively, and they are in good agreement with the predictions.

More recently, Komori *et al.* (1991*a*) measured the instantaneous concentrations of two reacting species in the same shear-free grid-generated turbulence as used in Komori *et al.* (1989). They used a rapid reaction between acetic acid (species *A*) and ammonium hydroxide (species *B*), and the Damköhler number Da_1 for the rapid reaction was 1.0×10^8 . Both species *A* and *B* had the same initial concentrations of 10 mol/m³ in water, and the laser dye (uranin) was premixed homogeneously in both streams. The lower (*A*) and upper (*B*) streams emerged into the test section at the same mean velocity of 0.25 m/s. The fluorescence was obtained by shooting a high-power argon-ion laser at the laser dye. The fluorescence intensity depended on the

local concentration of acetic acid and it decayed as the concentration of the acetic acid decreased. From this dependence, the concentration of the acetic acid (species A) was instantaneously measured. Instead of the concentration of the ammonium hydroxide (species B), the concentration of the chemical product was measured by using a single-electrode conductivity probe of $10\ \mu\text{m}$ diameter, and the concentration of species B was instantaneously derived from the mass conservation equation. This combined laser-induced fluorescence and electrode-conductivity technique enabled measurements to be made of two instantaneous concentrations of the species A and B , with smaller spatial resolution than the Kolmogorov microscale ($20\ \mu\text{m}$ for the laser-induced fluorescence technique and $40\ \mu\text{m}$ for the electrode-conductivity technique), and the resolution was a little larger than the Batchelor scale l_c ($15\ \mu\text{m}$ at $x/M = 20$). The details of this technique are described in Komori, Kanazaki & Murakami (1991*b*).

The new measurements of Komori *et al.* (1991*a*) are shown by open circles in figures 6, 8 and 11. Predictions using the flow and reaction properties given in table 2 are also shown by a dot-dash-line in the figures. As mentioned in §3.1, the case of very rapid reaction where $Da_1 = 1.0 \times 10^8$ corresponds to the limit where the assumptions of the present model are not satisfied. Not surprisingly the comparison between the measurements and the predictions shows the limitations of the present model. When we compare the mean concentration of species A with the prediction in figure 8, we see clearly that the reaction rate is underestimated, as anticipated in §3.1. However, even in this limiting case the maximum error in \bar{C} is only about 25%, and also it is found that the effect of the reaction between the marked particle and the ambient particles does not appear to be significant for a considerable distance along the mixing region (for $t/T_L \lesssim 10$). This means that over this distance the interface is still approximately continuous and does not contain significant cut-off regions, as shown in the photographs of figures 7 and 14. The segregation parameter α is scattered around the value of -1 . It is interesting that, despite the error in \bar{C} , the value of α predicted from the model is also equal to about -1 . The correlation coefficient R_{AB} between concentration fluctuations c_A and c_B increases with increasing t/T_L , and the measurements are also in qualitative agreement with the predictions. The deviation of R_{AB} from the predictions increases when t/T_L increases, since the reaction is significantly underestimated in the far mixing region at large t/T_L . However, the maximum error of R_{AB} at $t/T_L \sim 10$ can be estimated from figure 11 to be about 20%.

Thus, the new experiments of Komori *et al.* (1989 and 1991*a*) suggests that the present Lagrangian Stochastic model provides a useful estimate and qualitative insight into these kinds of turbulent flows, even when $Da_1 \gg 1$.

4.5. Discussion of previous experimental measurements of the segregation parameter α

In order to compare the predictions of the segregation parameter α with the previous measurements in reacting flows with moderately fast reactions reviewed in §2, the flow and reaction properties which appeared in (13) and (14) of the present Lagrangian stochastic model were set to match the experimental conditions. The properties used are listed in table 2. Here some of the previous measurements reviewed in §2, which have not shown all of the properties required for the model simulation, are excluded. For the three sets of experiments of Komori & Ueda (1984), Bennani *et al.* (1985) and Komori *et al.* (1989) in grid-generated turbulent flows, the measurements at the furthest upstream location were adopted, and the lengthscale

Parameters	Komori & Ueda (1984)		Mudford & Bilger (1984)	Komori <i>et al.</i> (1985)	Bennani <i>et al.</i> (1985)	Komori <i>et al.</i> (1989)	Komori <i>et al.</i> (1989)
	6.0×10^{-1}	3.4×10^{-1}	4.7×10^{-1}	5.0×10^{-1}	8.4×10^{-2}	1.9×10^{-2}	1.9×10^{-2}
	4.9×10^{-3}	1.1×10^{-2}	2.0×10^{-1}	8.1×10^{-1}	5.8×10^{-3}	3.3×10^{-3}	3.3×10^{-3}
	8.0×10^{-3}	3.2×10^{-2}	4.3×10^{-1}	1.6×10^0	6.9×10^{-2}	1.7×10^{-1}	1.7×10^{-1}
	4.4×10^1	3.6×10^0	5.1×10^{-1}	6.2×10^{-2}	1.0×10^{-1}	2.2×10^{-2}	2.2×10^{-2}
	0	9.0×10^{-1}	0	5.5×10^{-1}	0	0	0
	9.8×10^{-5}	1.8×10^{-4}	3.0×10^{-4}	5.1×10^{-4}	5.6×10^{-5}	7.6×10^{-5}	7.6×10^{-5}
	1.6×10^{-5}	1.6×10^{-5}	1.6×10^{-5}	1.6×10^{-5}	1.0×10^{-6}	1.0×10^{-6}	1.0×10^{-6}
	1.6×10^{-5}	1.6×10^{-5}	1.6×10^{-5}	1.6×10^{-5}	1.4×10^{-9}	1.7×10^{-9}	1.7×10^{-9}
	1.0×10^1	4.0×10^1	1.0×10^0	3.0×10^0	9.0×10^1	1.0×10^1	1.0×10^1
	(p.p.m.)	(p.p.m.)	(p.p.m.)	(p.p.m.)	(mol/m ³)	(mol/m ³)	(mol/m ³)
	2.0×10^0	2.0×10^0	1.0×10^0	6.0×10^{-2}	6.0×10^1	1.0×10^1	1.0×10^1
	(p.p.m.)	(p.p.m.)	(p.p.m.)	(p.p.m.)	(mol/m ³)	(mol/m ³)	(mol/m ³)
	3.8×10^{-1}	3.8×10^{-1}	3.8×10^{-1}	3.8×10^{-1}	4.7×10^{-2}	0	1.0×10^1
	(p.p.m. ⁻¹)	(p.p.m. ⁻¹ s ⁻¹)	(p.p.m. ⁻¹ s ⁻¹)	(p.p.m. ⁻¹ s ⁻¹)	(m ³ mol ⁻¹ s ⁻¹)		(m ³ mol ⁻¹ s ⁻¹)
	1.8×10^2	2.3×10^2	5.9×10^3	2.5×10^4	4.8×10^2	6.4×10^1	6.4×10^1
	1.0×10^0	1.0×10^0	1.0×10^0	1.0×10^0	7.0×10^2	6.0×10^2	6.0×10^2
	0-13.3	0-36.8	3.3-9.5	8.8, 25	3.6-12.3	1.4-9.6	2.4-

TABLE 2. Flow and reaction properties used in the present calculations for the comparisons with the measurements

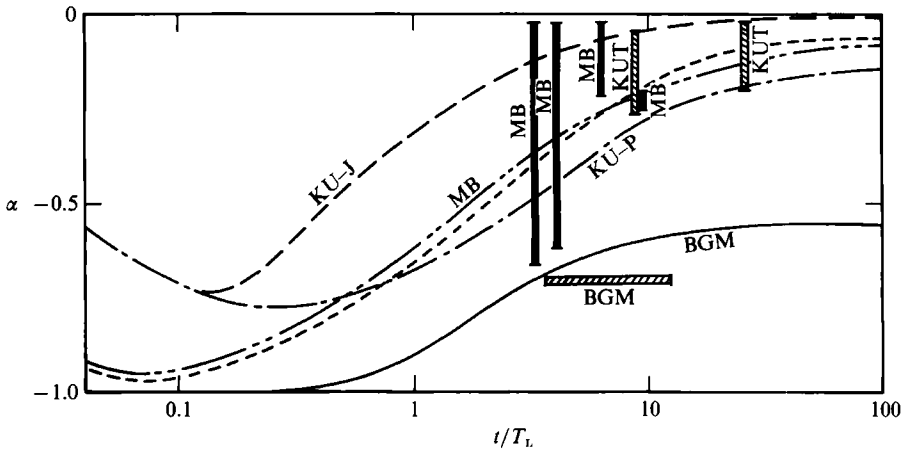


FIGURE 15. Comparisons of the segregation parameter α between the predictions and the previous measurements listed in table 2: KU-P, round plume in a grid-generated turbulence (Komori & Ueda 1984); KU-J, round jet in an irrotational coflow (Komori & Ueda 1984); MB, counter jets in a turbulent smog chamber (Mudford & Bilger 1984); KUT, two-dimensional plume in the atmospheric surface layer (Komori *et al.* 1985); BGM, homogeneous plume in grid-generated liquid turbulence (Bennani *et al.* 1985).

L and viscous dissipation were estimated by (28) and (29). For the experiments of Mudford & Bilger (1984), the averaged values of the measurements reported in their paper were used and the viscous dissipation was estimated by (29). For the observations in the atmospheric surface layer by Komori *et al.* (1985), the viscous dissipation and the lengthscale were estimated from the turbulence statistics measured by Hunt, Kaimal & Gaynor (1985) (specifically their equations (2) and (3)). The measurement range of each work was defined by using a non-dimensional relative time t/T_L on the assumption that the mean velocity U is constant. For the counter jets of Mudford & Bilger (1984), a stagnation point where the two jets begin to meet each other was taken as the origin of t/T_L and a value of t/T_L was estimated along the x -axis.

Figure 15 shows the predictions of the segregation parameter α for five reacting flows in table 2. For the reacting plume of Bennani *et al.* (1985) in grid-generated liquid turbulence, the predicted value of α is little larger than the measurements, but it tends to settle to a constant value of about 0.55 in the developed mixing region of $t/T_L > 10$. This behaviour is in good agreement with the measurements, though the constant value of -0.55 is larger than the measured value of -0.7 . Because this model requires a continuous interface which persists for longer, it is likely that the present model is in principle better for predicting the rather small values of α in liquid flow with a high Schmidt number than the higher values of α in gaseous flow with a low Schmidt number. Arrojo *et al.* (1988) have also modelled Bennani *et al.*'s (1985) measurements, but by using p.d.f. equations.

For the reacting counter jets of Mudford & Bilger (1984) with a low Schmidt number of $Sc = 1$, the values of α measured at four locations plotted against t/T_L have long data bands in the figure. The prediction curve (for their experimental condition when translated to homogeneous uniform flow) passes through their data bands except for the relative time of $t/T_L = 6.3$. In particular, the measured α at $t/T_L = 9.5$ is in good agreement with the prediction.

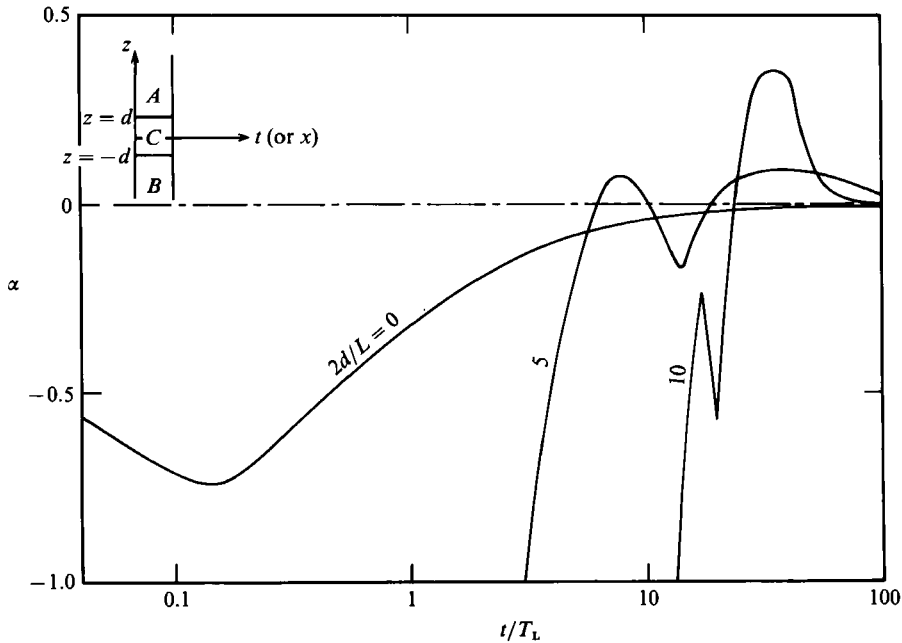


FIGURE 16. Initial concentration profile with three chemical species for a simulation of the effect of non-reactive chemical species C on the segregation parameter α for the reacting jet of Komori & Ueda (1984).

For the two-dimensional reacting plume of Komori *et al.* (1985) in the atmospheric surface layer, the values of α measured at two positions are scattered, like those of Mudford & Bilger (1984), but they seem to show a slight increase of α with the relative time of mixing t/T_L , again like Mudford & Bilger (1984). The predicted α also shows a similar increase, passing through the average of the measured α .

For the reacting round plume in grid-generated turbulence and the reacting jet with an irrotational coflow of Komori & Ueda (1984), the model predicts a negative value of α over the entire period of mixing. This prediction, which is consistent with the limits of α in (40) and (42), shows that the criticism by Bilger *et al.* (1985) of the measurements of Komori & Ueda (1984) is in one sense correct.

Here we have to explain why Komori & Ueda's (1984) measurements in a plume and a jet showed positive values of α . Komori & Ueda (1984) used a careful measuring procedure as mentioned in their paper and therefore it is difficult to admit the large measurement error suggested by Bilger *et al.* (1985). However, there is some doubt whether, in their experiments, the non-premixed condition was attained or not, i.e. whether the chemical species O_3 in their ambient coflow was homogeneously diluted by purified air to a scale less than the Kolmogorov scale η . In fact, their wind tunnels were not equipped with a method for thoroughly diluting O_3 .

The present model was used to simulate the effects of an initially inhomogeneous dilution by taking an idealized initial concentration profile with a non-reactive species C introduced between A and B in the range of $|z| < d$ (figure 16). The results in figure 16 show how α varies with time for the case of a reacting jet (Komori & Ueda 1984) with a non-reactive species. In this case the value of α has a maximum and becomes positive once the mixing has developed where $t/T_L \gtrsim 6$. The time for this

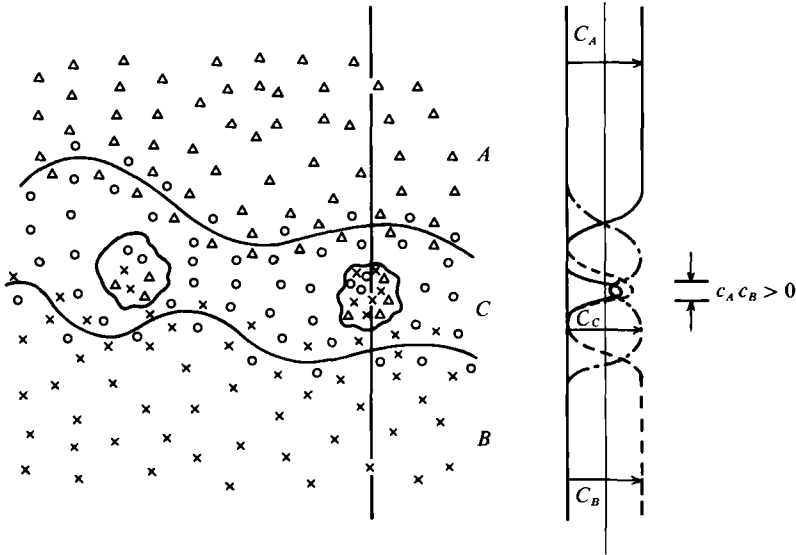


FIGURE 17. A physical mechanism for the mixing of three chemical species and their instantaneous concentration profiles.

transition depends on the spacing of C between species A and B in the initial concentration profile.

This situation is similar to Warhaft's (1984) experiments without reaction, where he introduced two non-reacting species into a grid-generated turbulent flow with a spacing d between the sources. Stapountzis (1988) repeated these measurements with shear. These experiments clearly showed that on the centreline between the sources α changes sign when the mixing time is greater than T_L . The exact time for this transition also depended on the spacing. (Detailed comparison of this flow with the two-particle model is given by Thomson 1990, while Picart *et al.* 1989 used direct numerical simulation to compute the time evolution of the correlation between c_A and c_B .) Based on the flow visualization study of Stapountzis (1988) one can say that, initially, the two species A and B are alternatively advected up and down by turbulent motions across $z = 0$, which leads to $\alpha < 0$. But further downstream, the interface becomes convoluted and pockets of unmixed A and B species are found in the volume occupied by non-reactive species C , as shown in figure 17. These processes (and lack of mixing) can generate a positive correlation between the concentration fluctuations of the two species, as shown by the instantaneous concentration profiles of figure 17. Thus, both the simulations and the measurements suggest that Komori & Ueda (1984) failed not in measuring the mean concentrations but in homogeneously diluting the chemical species at $t = 0$.

5. Concluding remarks

Since the ultimate stage of the mixing process is the transfer of matter or heat between fluid volumes by molecular processes, this process occurs at very small scales in turbulent flows with high Reynolds numbers. Mixing first requires large-scale motions bringing the volumes together (which is most easily understood in Lagrangian terms), and then it involves small-scale-motion processes where molecular diffusion between high concentration and low concentration in the fluid

volumes is of the same order as the local transport by the local straining motions. (This process is best understood in Eulerian terms – in a frame of reference moving with the large eddies.)

So models must allow for both the large-scale and small-scale processes. However, as usual in turbulence, most models invoke some assumptions that the small-scale processes are determined by the large-scale motions and are independent of the Schmidt number. But they are not in general valid for mixing processes, since the small scales can play an important role, except for extremely high Reynolds numbers. We have described one kind of model based on two-particle trajectories plus small-scale mixing, and we have applied the model to a non-premixed reacting flow with a moderately fast or slow second-order reaction.

The main conclusions from the simulations by our model can be summarized as follows.

(i) The relative mixing time t/T_L , the turbulent Reynolds number Re_t , the Schmidt number Sc , the Damköhler number based on the integral timescale Da_1 and the ratio of the initial concentrations β are the important parameters which determine the segregation parameter α , and therefore the mean chemical reaction rate in a non-premixed reacting flow (in a process where Da_1 is of order unity). By estimating these five parameters, the present model enables us to indicate an approximate value for the segregation parameter α . Also, it can qualitatively explain most previous measurements of the segregation parameter, about which there has been substantial disagreement among experimentalists.

(ii) In the initial region near the source, the segregation parameter is negative and it grows towards zero with increasing mixing time. The growing rate for $Sc \sim 1$ is larger than for $Sc \sim 10^3$. For a high Damköhler number, the segregation parameter remains at a large negative value, even for a large mixing time, and therefore for a large mixing time the chemical reaction rate decreases in the downstream region. The variations of the segregation parameter with the mixing time can also be explained by a physical mechanism based on the motion of the interface.

(iii) Shear can rapidly increase the segregation parameter towards zero, and therefore promote the chemical reaction rate even for a high Damköhler number.

Strictly, these results are limited to low-shear or shear-free turbulence with a moderately fast or slow reaction and the reacting zone near the source, because of the assumption used in the model. Therefore, applying the model to larger mixing times or higher shear rates may lead to some errors due to underestimating the amount and the rate of the reaction.

In the future there should be an improvement in Lagrangian methods resulting from direct simulation of turbulent flows and the computations of trajectories using large computers (e.g. Girimaji & Pope 1990) or by large-eddy or possibly 'kinematic simulations' (Drummond & Münch 1990; Malik 1990; Canuto *et al.* 1990). In particular it will be interesting to see computations of relative diffusion (cf. ensembles of pairs and larger groups) and the comparison with simple stochastic models (such as (11)). Even when Lagrangian trajectories are better understood and better modelled, they still have to be related to the small-scale molecular diffusion processes (e.g. Canuto *et al.* 1990). Computations and simulations of Lagrangian trajectories will also help other kinds of modelling, notably those based on assumed forms of probability distributions.

The authors gratefully acknowledge the financial support for this study by the NISSAN Science Foundation and Japanese Grant-in-Aid for Scientific Research on Priority Areas 'Exploration of Combustion Mechanism'. S.K. would like to thank

the Japan Society for the Promotion of Science for granting the financial support for his stay in Cambridge under the Royal Society's agreement on scientist exchange. Much of the initial research at Cambridge into mixing has been within the Wolfson Group supported by the Wolfson Foundation. We are grateful for useful conversations and corresponds with Drs H. Ueda, R. Bilger, R. E. Britter, P. Durbin, N. Peters, S. B. Pope, B. Sawford, E. Stapoutzis, Z. Warhaft, and the referees.

REFERENCES

- ARROJO, P., DOPAZO, C., VALINO, L. & JONES, W. P. 1988 Numerical simulation of velocity and concentration fields in a continuous flow reactor. *Chem. Engng Sci.* **43**, 1935–1940.
- BATCHELOR, G. K. 1952 Diffusion in a field of homogeneous turbulence II. The relative motion of particles. *Proc. Camb. Phil. Soc.* **48**, 345–362.
- BENNANI, A., GENGE, J. N. & MATHIEU, J. 1985 The influence of a grid-generated turbulence on the development of chemical reactions. *AIChE J.* **31**, 1157–1166.
- BILGER, R. W., MUDFORD, N. R. & ATKINSON, J. D. 1985 Comments on 'Turbulent effects on the chemical reaction for a jet in a nonturbulent stream and for a plume in a grid-generated turbulence'. *Phys. Fluids* **28**, 3175–3177.
- BOURNE, J. R., KOZICKI, F., MOERGELI, U. & RYS, P. 1981 Mixing and fast chemical reaction – III. *Chem. Engng Sci.* **36**, 1655–1663.
- BROADWELL, J. E. & BREIDENTHAL, R. E. 1982 A simple model of mixing and chemical reaction in a turbulent shear layer. *J. Fluid Mech.* **125**, 397–410.
- CANUTO, U. M., HARTKE, C. J., BERTOGLIO, A., CHASNOV, J. & ALBRECHT, G. F. 1990 Theoretical study of turbulent channel flow: bulk properties, pressure fluctuations and propagations of electromagnetic waves. *J. Fluid Mech.* **211**, 1–35.
- CHUNG, P. M. 1976 A kinematic-theory approach to turbulent chemically reacting flows. *Combust. Sci. Technol.* **13**, 123–153.
- CORRSIN, S. 1952 Heat transfer in isotropic turbulence. *J. Appl. Phys.* **23**, 113–118.
- CURL, R. L. 1963 Dispersed phase mixing: I. Theory and effects in simple reactors. *AIChE J.* **9**, 175–181.
- DANCKWERTS, P. V. 1952 The definition and measurement of some characteristics of mixtures. *Appl. Sci. Res. A* **3**, 279–296.
- DRUMMOND, I. T. & MÜNCH, W. H. P. 1990 Turbulent stretching of lines and surfaces. In *Topological Fluid Mechanics*, pp. 628–636. Cambridge University Press.
- DURBIN, P. A. 1980 A stochastic model of two-particle dispersion and concentration fluctuations in homogeneous turbulence. *J. Fluid Mech.* **100**, 279–302.
- DURBIN, P. A. 1989 A Lagrangian theory of turbulent nonpremixed reacting flow. *J. Fluid Mech.* (submitted).
- GIBSON, C. H. & LIBBY, P. A. 1972 On turbulent flows with fast chemical reactions. The distribution of reactors and products near a reacting surface. *Combust. Sci. Technol.* **6**, 29–35.
- GIRIMAJI, S. S. & POPE, S. B. 1990 Material-element deformation in isotropic turbulence. *J. Fluid Mech.* **220**, 427–458.
- HILL, J. C. 1976 Homogeneous turbulent mixing with chemical reaction. *Ann. Rev. Fluid Mech.* **8**, 135–161.
- HUNT, J. C. R., KAIMAL, J. C. & GAYNOR, J. E. 1985 Some observations of turbulence structure in stable layers. *Q. J. R. Met. Soc.* **111**, 793–815.
- KOMORI, S., KANZAKI, T. & MURAKAMI, Y. 1991a Concentration statistics in shear-free grid-generated turbulence with a second-order rapid reaction. In *Advances in Turbulence 3* (ed. A. Johansson & H. Alfredsson). Springer (in press).
- KOMORI, S., KANZAKI, T. & MURAKAMI, Y. 1991b Simultaneous measurements of instantaneous concentrations of two reacting species in a turbulent flow with a rapid reaction. *Phys. Fluids A* **3**, 507–510.
- KOMORI, S., KANZAKI, T., MURAKAMI, Y. & UEDA, H. 1989 Simultaneous measurements of instantaneous concentrations of two species being mixed in a turbulent flow by using a

- combined laser-induced fluorescence and laser-scattering technique. *Phys. Fluids A* **1**, 349–351.
- KOMORI, S. & UEDA, H. 1984 Turbulent effects on the chemical reaction for a jet in a nonturbulent stream and for a plume in a grid-generated turbulence. *Phys. Fluids* **27**, 77–86.
- KOMORI, S., UEDA, H. & TSUKUSHI, F. 1985 Turbulent effects on the chemical reaction in the atmospheric surface layer. In *Proc. 50th annual meeting of the Japanese chemical engineers*, pp. 241 (in Japanese) unpublished.
- LIBBY, P. A. & WILLIAMS, F. A. 1980 *Turbulent Reactive Flows*. Springer.
- MALIK, N. A. 1990 Distortion of material surfaces in steady and unsteady flows. In *Topological Fluid Mechanics*, pp. 617–627, Cambridge University Press.
- MUDFORD, N. R. & BILGER, R. W. 1984 Examination of closure models for mean chemical reaction rate using experimental results for an isothermal turbulent reacting flow. In *Twentieth Symposium on Combustion*, pp. 387–394. The Combustion Institute.
- PICART, A., CHOLLET, J. P. & BORGHINI, R. 1989 Turbulent diffusion from thermal or reactive sources: numerical experiment. In *Advances in Turbulence 2* (ed. H. H. Fernholz & H. E. Fiedler), pp. 192–197. Springer.
- POPE, S. B. 1985 PDF methods for turbulent reactive flows. *Prog. Energy Combust. Sci.* **11**, 119–192.
- RILEY, J. J., METCALFE, R. W. & ORSZAG, S. A. 1986 Direct numerical simulations of chemically reacting turbulent mixing layers. *Phys. Fluids* **29**, 406–421.
- SAETRAN, L. R., HONNERY, D. R., STARNER, S. H. & BILGER, R. W. 1989 Scalar mixing layer in grid turbulence with transport of passive and reactive species. In *Turbulent Shear Flow 6* (ed. F. J. Durst, B. E. Launder, F. W. Schmidt & J. H. Whitelaw), pp. 109–118. Springer.
- SAFFMAN, P. G. 1960 On the effect of the molecular diffusivity in turbulent diffusion. *J. Fluid Mech.* **3**, 273–283.
- SAWFORD, B. L. 1984 Reply to comments by Egbert and Baker. *Q. J. R. Met. Soc.* **110**, 1199–1200.
- SAWFORD, B. L. 1985 Lagrangian statistical simulation of concentration mean and fluctuation fields. *J. Climate Appl. Met.* **24**, 1152–1166.
- SAWFORD, B. L. & HUNT, J. C. R. 1986 Effects of turbulence structure, molecular diffusion and source size on scalar fluctuations in homogeneous turbulence. *J. Fluid Mech.* **165**, 373–400.
- STAPOUNTZIS, H. 1988 Covariance and mixing of temperature fluctuations from line sources in grid turbulence. In *Transport Phenomena in Turbulent Flows* (ed. M. Hirata & N. Kasagi), pp. 419–431. Hemisphere.
- STAPOUNTZIS, H. & BRITTER, R. E. 1989 Turbulent diffusion behind a heated line source in a nearly homogeneous turbulent shear flow. In *Turbulent Shear Flow 6* (ed. F. J. Durst, B. E. Launder, F. W. Schmidt & J. H. Whitelaw), pp. 97–108. Springer.
- STAPOUNTZIS, H., SAWFORD, B. L., HUNT, J. C. R. & BRITTER, R. A. 1986 Structure of the temperature field downwind of a line source in grid turbulence. *J. Fluid Mech.* **165**, 401–424.
- TAYLOR, G. I. 1921 Diffusion by continuous movements. *Proc. Lond. Math. Soc.* (2) **20**, 196–212.
- THOMSON, D. J. 1986 On the relative dispersion of two particles in homogeneous stationary turbulence and the implications for the size of concentration fluctuations at large times. *Q. J. R. Met. Soc.* **112**, 890–894.
- THOMSON, D. J. 1990 A stochastic model for the motion of particle pairs in isotropic high-Reynolds-number turbulence, and its application to the problem of concentration variance. *J. Fluid Mech.* **210**, 113–153.
- TOOR, H. L. 1969 Turbulent mixing of two species with and without chemical reaction. *Indust. Engng Chem. Fundam.* **8**, 655–659.
- WARHAFT, Z. 1984 The interference of thermal fields from line sources in grid turbulence. *J. Fluid Mech.* **114**, 363–387.